CORA Cork Open Research Archive
Cartlann Taighde Oscailte Chorcaí

Title	Green chemistry approaches to the depolymerisation of polyolefin plastic packaging
Authors	Yap, Forest Tung Jie
Publication date	2025
Original Citation	Yap, F. T. J. 2025. Green chemistry approaches to the depolymerisation of polyolefin plastic packaging. MRes Thesis, University College Cork.
Type of publication	Masters thesis (Research)
Rights	© 2025, Forest Tung Jie Yap. - https://creativecommons.org/licenses/by/4.0/
Download date	2026-11-07 12:11:27
Item downloaded from	https://hdl.handle.net/10468/18433

UCC
University College Cork, Ireland
Coláiste na hOllscoile Corcaigh

Ollscoil na hÉireann, Corcaigh

National University of Ireland, Cork



Green Chemistry Approaches to the Depolymerisation of Polyolefin Plastic Packaging

Thesis presented by

Forest Tung Jie Yap, BSc.

for the degree of

Master of Research

University College Cork

School of Chemistry

Head of School: Prof. Anita Maguire

Supervisor: Dr. Gillian Collins

2025

Table of contents

Declaration ..... **IV**

List of Abbreviations ..... **V**

Acknowledgements ..... **VIII**

Abstract ..... **IX**

List of Figures ..... **X**

List of Tables ..... **XV**

Nomenclature ..... **XVI**

1 Chapter 1: Introduction **1**

1.1 Background 2

1.2 Overview of Polymer Types 4

1.3 Recycling Pathways for Plastic Waste 6

1.4 Post-Consumer Plastic and Plastic Additives 9

2 Chapter 2: Experimental **16**

2.1 Introduction 17

2.2 Fourier-transform infrared (FTIR) spectroscopy 17

2.3 X-ray photoelectron spectroscopy (XPS) 19

2.4 High performance liquid chromatography (HPLC) 20

2.5 Thermo-Oxidative Reactions: Carousel 12 Plus Reaction Setup™ 22

2.6 Catalyst Preparation 24

2.6.1 Homogeneous catalyst 24

2.6.2 Fe_2O_3 (hematite) 24

2.6.3 Fe-CeO_2 catalyst 25

2.6.4 $MnFe_2O_4$ catalyst 25

2.6.5 $CoFe_2O_4$ catalyst 26

3 Chapter 3: Results & Discussion 27

3.1 Introduction 28

3.1.1 Research Aims and Objectives 28

3.2 Method development 30

3.2.1 Development of Reaction Apparatus 30

3.2.2 Initial catalyst screening 31

3.2.3 Comparing the effects of oxidative thermal-catalytic treatment on pristine LDPE resin and post-consumer LDPE film 37

3.2.4 Time Optimisation of the Degradation Reaction 43

3.2.5 Catalyst and NHPI Loading 46

3.2.6 Probing Oxidant Availability with Hydrogen Peroxide (H_2O_2) 50

3.3 Effect of a Second Thermal Treatment 52

3.4 High Performance Liquid Chromatography (HPLC) Analysis 55

3.4.1 Effect of Mn–Fe heterogeneous catalyst and NHPI loading on product distribution for PC-LDPE 61

3.4.2 Second Acetolysis Treatment 64

3.5 X-Ray Photoelectron Spectroscopy (XPS) Analysis 66

4 Chapter 4: Conclusions & Outlook 72

4.1 Conclusions 73

4.2 Future Work 75

Bibliography 78

Declaration

This is to certify that I, Forest Tung Jie Yap, am submitting work that is my own and has not been submitted for another degree, either at University College Cork or elsewhere. All external references and sources are clearly acknowledged and identified within the contents. I have read and understood the regulations of University College Cork concerning plagiarism and intellectual property.

Forest Tung Jie Yap

Forest Tung Jie Yap

List of Abbreviations

Abbreviation	Meaning
ABS	Acrylonitrile butadiene styrene
APP	Ammonium phosphates
ATR-FTIR	Attenuated total reflectance Fourier-transform infrared
BBP	Butyl benzyl phthalate
BE	Binding energy
BET	Brunauer-Emmett-Teller
BHT	Butylated hydroxytoluene
CI	Carbonyl index
CRM	Chemical recycling to monomer
DBP	Di n-butyl phthalate
DEHP	Di(2-ethyl hexyl) phthalate
DEPAL	Aluminium diethylphosphinate
DI	Deionised
DINP	Diisononyl phthalate
DOP	Dioctylphthalate
DTGS	Deuterated triglycine sulfate
EDX	Energy-dispersive X-ray spectroscopy
EG	Expandable graphite
EoL	End-of-life
EPS	Expanded polystyrene
GC-MS	Gas chromatography-mass spectrometry

GHG	Greenhouse gases
HALS	Hindered amine light stabilisers
HDPE	High-density polyethylene
HIPS	High impact polystyrene
HPLC	High performance liquid chromatography
KE	Kinetic energy
LDPE	Low density polyethylene
LLDPE	Linear low-density polyethylene
MAH	Maleic anhydride
mAu	milli-Absorbance units
MC	Mid-Century
Mt	Million metric tonnes
NHPI	N-Hydroxy phthalimide
NIR	Near-infrared
PC	Post-consumer
PC-LDPE	Post-consumer low density polyethylene
PET	Polyethylene terephthalate
PHA	Polyhydroxyalkanoates
PINO	Phthalimide N-oxyl
PLA	Polylactic acid
PP	Polypropylene
PS	Polystyrene
PTFE	Polytetrafluoroethylene
PU	Polyurethane

PVC	Polyvinyl chloride
RIC	Resin identification code
RT	Retention time
SAUB	Specific area under band
SEM	Scanning electron microscopy
SPE	Solid-phase extraction
TBBPA	Tetrabromobisphenol A
Tg	Glass transition temperature
TGA	Thermogravimetric analysis
UV	Ultraviolet
UVAs	UV absorbers
V-LDPE	Virgin low density polyethylene
XPS	X-ray photoelectron spectroscopy
XRD	X-ray diffraction

Acknowledgements

First and foremost, I would like to thank my supervisor Dr. Gillian Collins for the opportunity to undertake this research master's as well as her consistent guidance and support throughout the project. Without her, none of this research would have been possible.

Thank you to the programme director Dr. Brenda Long for her encouragement and support throughout the registration process. A big thanks also to all the administration staff and technical staff in UCC, especially in the school of chemistry for their assistance throughout the year. The school would be chaos without you.

To the Gillian Collin's collective—of which I am so proud to be a part—Rachel, Doireann, Rebecca and Clodagh, for being such an amazing group not only to work with, but also to share many laughs with. A special thank you to Rachel (soon to be Dr!) for all her help and mentoring during my research journey here. Many thanks also to my colleagues in lab 115 and 320, and to the lunch group for daily chats and our multinational table of treats.

A big thank you to my friends: Rebecca, Ula, Tara and Jack, for being there in my time of need in undergrad (specifically final year) as well as during my master's. And to Marjorie, Khushboo and Aoife—thank you for truly making college the best four years of my life.

Finally, my heartfelt gratitude to my mom and dad for their endless sacrifices, to my sisters, Chloe and Rachel, and to my dearest grandma for their unconditional love and support throughout my life. Without them all, I would not be the person that I am today.

Abstract

The widespread use of polyolefin plastic packaging has contributed significantly to the global plastic waste crisis, posing severe environmental and economic challenges, making the development of effective plastic degradation strategies imperative for sustainable waste management. This thesis investigates the thermo-oxidative degradation of both virgin (V-) and post-consumer (PC-) low-density polyethylene (LDPE) in acetic acid under relatively mild conditions (120 °C, ambient pressure), evaluating the roles of heterogenous Mn-Fe catalysts, N-Hydroxyphthalimide (NHPI) radical initiator and catalyst-free degradation. Across all experimental conditions PC-LDPE consistently exhibited greater mass loss (~30 %) than V-LDPE (~17 %). Surface-sensitive characterisation by Fourier-transform infrared spectroscopy and X-ray photoelectron spectroscopy revealed a significantly higher degree of functionalisation for PC-LDPE than V-LDPE, attributed to prior oxidation and additives in post-consumer plastics. Qualitative analysis using HPLC consistently showed the presence of formic acid and succinic acid as major degradation products with additional minor signals also observed in the PC-LDPE. The presence of additives and prior processing history have a strong influence on the degradation pathways of LDPE. We further show that heating in acetic acid alone can drive partial thermo-oxidative conversion of PC-LDPE under mild catalyst-free conditions (120 °C, acetic acid). This approach presents opportunities for designing a mild oxidative pretreatment of PC-LDPE that could be coupled to a subsequent harsher chemical upcycling process.

List of Figures

Figure 1. European plastics production of different plastics. Polyethylene terephthalate (PET), high density polyethylene (HDPE), low-density polyethylene (LDPE), polypropylene (PP), polystyrene (PS), polyvinyl chloride (PVC), polyurethane (PUR) and other plastics[11]. 3

Figure 2. Common classification of usual recycling strategies for plastic wastes. Figure has been reproduced from ref[20]. 7

Figure 3. Schematic representation of an ATR-FTIR system reproduced from ref[51]. 18

Figure 4. Schematic representation of the XPS process reproduced from ref[52]. 20

Figure 5. HPLC setup used and schematic for the mechanism of size exclusion column reproduced from ref[54]. 22

Figure 6. (a) Carousel 12 Plus Reaction Station™ setup with (b) glass tube and PTFE cap. 24

Figure 7. Schematic of the degradation mechanism. a) Conversion of NHPI to active species, PINO. b) Proposed pathway for the oxidative degradation of LDPE using NHPI and metal catalysts in the presence of O_2. 32

Figure 8. SEM micrograph and corresponding EDX of the Fe-CeO_2 catalyst. The SEM image reveals the surface morphology, while the EDX analysis confirms the presence of Fe, Ce and O distributed evenly within the material. 34

Figure 9. SEM micrograph and corresponding EDX of the Mn-Fe catalyst. The SEM image shows a heterogeneous surface morphology, while the EDX analysis confirms the presence of Mn, Fe and O evenly distributed within the material, consistent with the intended mixed- metal composition. 35

Figure 10. Effect of overnight stirring in acetic acid on LDPE mass loss for different catalytic systems. General variability in mass loss was obtained from a set of key reference reactions (see Experimental Section for further details). The mean mass loss for V-LDPE was 6 ± 10 %, n=3, while the mean mass loss for PC-LDPE was 30.9 ± 2 %, n=3. 36

Figure 11. The effect of congealing on mass loss. Unlike PC-LDPE which does not congeal, when V-LDPE undergoes thermal treatment in the absence or presence of catalyst and NHPI, it will either congeal or remain dispersed in solution. However, once congealing occurs, the surface becomes deactivated and prevents further reaction. 38

Figure 12. FTIR spectra of unreacted virgin LDPE (V-LDPE) and post-consumer LDPE (PC-LDPE) with characteristic PE bands. 39

Figure 13. FTIR spectra of virgin LDPE after reaction with homogeneous (Co/ Mn acetate) and heterogeneous ($CoFe_2O_4$) catalysts. Sample treated with homogeneous catalyst (blue line) showed no functionalisation, whereas LDPE reacted with a heterogeneous catalyst (black line) exhibits clear peaks in the carbonyl region (1718 and 1627 cm^{-1}), along with weak bands in the C-O stretching region (1200-900 cm^{-1}), indicating oxidative functionalisation of the polymer. 40

Figure 14. FTIR spectra of virgin and post-consumer LDPE after reaction with the same homogeneous catalyst (Co and Mn acetate). The virgin LDPE shows no evidence of chemical functionalisation, while post-consumer LDPE displays a sharp N-H stretching peak (3500-3300 cm^{-1}), O-H band (3100-3000 cm^{-1}), carbonyl peaks (1800-1500 cm^{-1}), and C-O stretching bands (1260-900 cm^{-1}), consistent with the formation of carboxylic acid functional groups. 41

Figure 15. Comparative FTIR spectra of post-consumer LDPE reacted with $MnFe_2O_4$ heterogeneous catalyst at 120 ^oC over varying time intervals. Left: unreacted PC-LDPE (black), 5 h (blue), 8 h (red); right: 15 min (green), 30 min (orange), 1 h (blue), 2 h (yellow), and 3 h (purple). 45

Figure 16. FTIR spectra of LDPE before (black) and after reaction with different catalyst loadings: 0 wt% (blue), 5 wt% (green), 9.6 wt% (yellow), and 15 wt% (red) shows increasing oxidation with decreasing catalyst loading and that the highest degree of functionalisation stems from reaction with no catalyst. A corresponding decrease in CH_2 stretching peaks suggests progressive breakdown of the polymer backbone during oxidation. 48

Figure 17. FTIR spectra of LDPE following reaction at 120 °C for 5 h (fixed Mn-Fe catalyst loading) reacting with varying NHPI loading: 0 wt%, 11.2 wt% and 20 wt%. Despite similar bulk mass loss (~30 %) across all samples, the highest oxidation was observed in the control (no NHPI), minimal levels at 11.2 wt% and intermediate levels at 20 wt% NHPI. 49

Figure 18. FTIR spectra of PC-LDPE after 1 h reactions under different conditions: control without peroxide (blue line), peroxide added as single initial dose (red line), peroxide added incrementally with analysis of two different areas of the same sample (green and yellow line)..... 52

Figure 19. Effect of a second thermo-oxidative treatment on PC-LDPE under different conditions: **(a)** 5 h, catalyst, NHPI; **(b)** 1 h, catalyst, NHPI; **(c)** 1 h, no catalyst or NHPI. In the presence of catalyst and NHPI, the emergence of a new peak 1739 cm^{-1} was observed indicating a shift to more thermodynamically stable carbonyl species. While

in the absence of catalyst and NHPI, only lower intensity peaks were seen after the second cycle. 53

Figure 20. Calibration curves for the different carboxylic acids obtained from HPLC. All curves exhibited good linearity across the calibration range. 56

Figure 21. Qualitative HPLC chromatograms comparing the products of V-LDPE after reaction with two different catalysts. **(A)** homogeneous Co/Mn acetate catalyst and **(B)** heterogeneous Co-Fe catalyst. 59

Figure 22. Qualitative HPLC chromatogram of PC-LDPE after reaction with homogeneous Co/Mn acetate catalyst. 60

Figure 23. Qualitative comparison of HPLC chromatograms for PC-LDPE showing **(A)** the absence and presence of an impurity peak at lower (5 wt%) and higher (15 wt%) catalyst loadings, respectively, and **(B)** the effect of different catalyst loadings on the product distribution after reaction. Increasing catalyst loading seem to increase the product profile with the most compounds being identified at 9.6 and 15 wt% Mn-Fe catalyst. 62

Figure 24. Qualitative HPLC chromatogram of PC-LDPE after a reaction **(a)** with no catalyst or NHPI and **(b)** with catalyst and NHPI. Both showing a narrow product distribution with formic acid at 17.2 min and an unresolved peak at 21-22 min. 63

Figure 25. Schematic representation of a typical PC-LDPE run showing the distribution of mass into recovered solid, quantified carboxylic acids, dissolved unassigned products, and collected volatiles. 66

Figure 26. Survey XPS spectra for virgin and post-consumer LDPE samples before reaction (control) and after a 15 min and 3 h reaction. Post-reaction samples have been washed with DI H_2O prior to XPS analysis..... 67

Figure 27. (a) C 1s XPS, **(b)** O 1s XPS and **(c)** FTIR analysis for virgin LDPE before and after a 3 h reaction. All samples have been washed with DI H_2O prior to XPS analysis. 69

Figure 28. (a) C 1s XPS, **(b)** O 1s XPS and **(c)** N 1s XPS for post-consumer LDPE before reaction and after a 15 min and 3 h reaction. FTIR analysis of PC-LDPE samples after **(d)** 15 min and **(e)** 3 h..... 70

List of Tables

Table 1. Types of plastic, their resin identification codes (RICs), and chemical structures. 5

Table 2. Common types of additives used in the manufacture of plastics, examples, and their function in plastics. 12

Table 3. Summary of catalysts used for LDPE degradation experiments. 35

Table 4. The effect of reaction time on mass loss and carbonyl index (CI) of PC-LDPE. The mass loss reaches a fundamental plateau at ca. 30 % and the carbonyl index does not exhibit a consistent trend over time, fluctuating without clear correlation to reaction duration. 44

Table 5. Retention times in minutes for each end-product 57

Table 6. Reaction products detected after a first and second run of the acetolysis reaction with PC-LDPE, with more products generated after a second treatment of the polymer. 65

Table 7. Atomic concentrations (%) of the different elements constituting the surface of the virgin and post-consumer LDPE samples after a 15 min and 3 h reaction. 67

Nomenclature

Sample	Description (all reactions carried out at 120°C)	
V-LDPE	Virgin low-density polyethylene (LDPE)	
PC-LDPE	Post-consumer LDPE	
V-LDPE_unrxtd	V-LDPE before reaction	
PC-LDPE_unrxtd	PC-LDPE before reaction	
V-LDPE_homo	V-LDPE, Co/Mn/NHPI, 5 h	
V-LDPE_het	V-LDPE, $CoFe_2O_4$, NHPI, 5 h	
Effect of Time		
PC-LDPE_8h; 5h; 3h; 2h; 1; 30min; 15min	PC-LDPE, $MnFe_2O_4$ (9.6 wt%), NHPI (11.2 wt%), varying time intervals	
Effect of Catalyst Loading (wt%)		
PC-LDPE_C0; 5; 9.6; 15	PC-LDPE, NHPI (11.2 wt%), varying $MnFe_2O_4$ catalyst loading, 5 h	
Effect of NHPI loading (wt%)		
PC-LDPE_N0; 11.2; 20	PC-LDPE, $MnFe_2O_4$ (9.6 wt%), varying NHPI loading, 5 h	
Effect of H_2O_2		
PC-LDPE_control	No H_2O_2	$MnFe_2O_4$ (9.6 wt%), NHPI (11.2 wt%), 1 h
PC-LDPE_H_2O_2_inst	Instantaneous addition	
PC-LDPE_H_2O_2_incr	Incremental addition	
Effect of Second Treatment		
2PC-LDPE_T1	$MnFe_2O_4$ (9.6 wt%), NHPI (11.2 wt%), 5 h	
2PC-LDPE_T2	$MnFe_2O_4$ (9.6 wt%), NHPI (11.2 wt%), 1 h	
2PC-LDPE_T3	No catalyst or NHPI, 1 h	

Chapter 1

Introduction

Chapter 1:

Introduction

Plastics—a manufacturing revolution in the early 20th century that was not constrained by the limits of nature but instead driven by human ingenuity. Owing to its durability, versatility, stability, low manufacturing cost and light weight properties, plastics democratised consumer goods, providing a more accessible alternative for items previously made from scarce materials like horn, ivory, tortoiseshell and rubber[1,2].

1.1 Background

Plastics are found in diverse fields such as packaging, construction, medicine, household appliances, electronics, automotive and aerospace components. The rapid growth in global plastic production has been largely driven by the availability of fossil fuels, which serve as both the energy source and hydrocarbon feedstock for polymer synthesis. Currently, over 90% of plastics produced are derived from virgin fossil feedstocks which accounts for an estimated 4-6% of global oil consumption[3]. From the 1950s to early 2000s, the annual production of plastics experienced exponential growth from 1.5 million metric tonnes (Mt) to 245 Mt in 2008, increasing to 413.8 Mt in 2023, with the EU27+3 region, which includes the 27 European Union member states along with the United Kingdom, Norway and Switzerland, accounting for 12.3 % of global plastics production[4]. Despite the substantial benefits of plastics, widespread use is accompanied by significant drawbacks, including environmental persistence[5,6], bioaccumulation in ecosystems[7,8], and the emission of greenhouse

gases during both the production and degradation stage[9,10], all of which pose serious challenges to sustainability and climate objectives.

In Europe in 2020, approximately 17.9 Mt of plastics packaging waste was generated, of which 46 % was recycled, 37 % was recovered for energy, and the remaining 17 % was sent to landfill[11]. In 2021, global plastic production reached 390.7 Mt, with Europe accounting for approximately 15 % of this total, contributing 57.2 Mt[11]. As well as this, it was reported that the average amount of plastic packaging waste generated in Ireland was 232 kg per capita in 2022[12]. At the present rate of growth, the global production of thermoplastics alone is projected to reach nearly 600 Mt in 2050[13]. The relative quantities of the main polymer families produced are shown in Figure 1 where the polyolefins; PP, LDPE, and HDPE, collectively account for just over 40 % of the total mass, illustrating their central role in current recycling efforts.

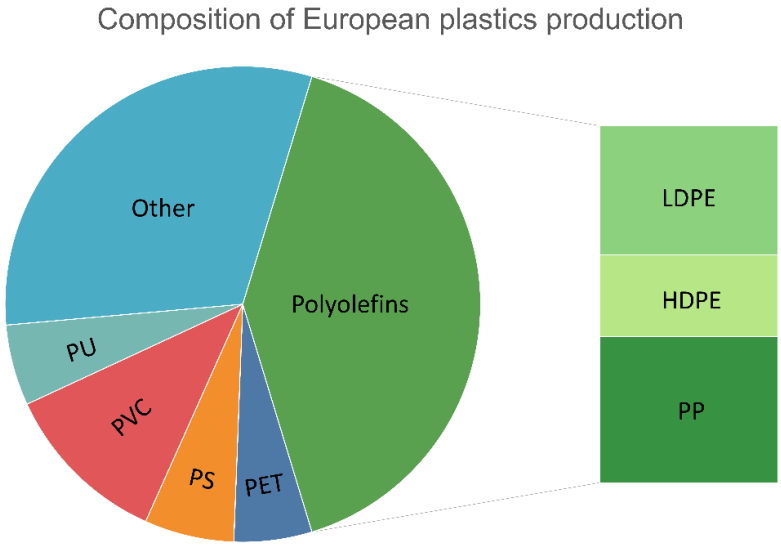


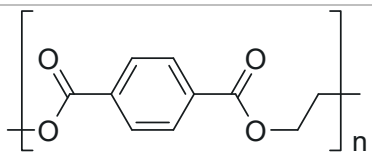
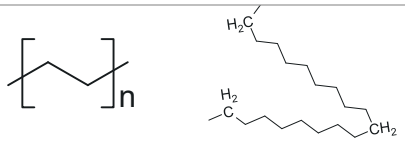
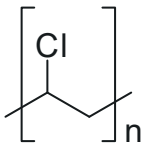
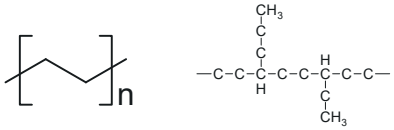
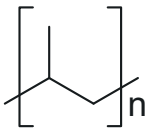
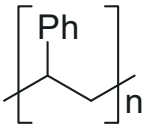
Figure 1. European plastics production of different plastics. Polyethylene terephthalate (PET), high density polyethylene (HDPE), low-density polyethylene (LDPE), polypropylene (PP), polystyrene (PS), polyvinyl chloride (PVC), polyurethane (PUR) and other plastics[11].

1.2 Overview of Polymer Types

Polymers are categorised by the Resin Identification Code (RIC) system, a standardised method developed to identify different types of plastic resins used in products and packaging. The system uses numbers 1 through 7, as shown in Table 1. Category 1 (Polyethylene Terephthalate, PET) is widely used for beverage bottles and food packaging due to its strength, clarity, and good barrier properties. Category 2 (High-Density Polyethylene, HDPE) is characterised by a linear structure with minimal branching, making it suitable for rigid containers such as detergent bottles and piping. Category 3 (Polyvinyl Chloride, PVC) incorporates chlorine atoms, conferring chemical resistance and rigidity, and is commonly used in construction materials and electrical insulation. Category 4 (Low-Density Polyethylene, LDPE) possesses a highly branched structure, resulting in flexibility which is well-suited for film applications like plastic bags and wraps. Category 5 (Polypropylene, PP) exhibits high thermal stability and is used extensively in packaging, medical devices, and automotive components. HDPE, LDPE and PP are members of the polyolefin family, a class of polymers produced from simple alkenes (olefins), such as ethylene and propylene, through coordination or free-radical polymerisation. Polyolefins are characterised by their hydrocarbon-based, non-polar backbones, contributing to their chemical inertness and wide applicability. Category 6 (Polystyrene, PS)—while not a polyolefin by strict chemical classification due to the presence of aromatic phenyl side groups—shares some similarities in synthesis and processing behaviour with polyolefins and is a rigid or foamed aromatic polymer widely used in disposable cutlery, insulation, and packaging.

Category 7 plastics are a miscellaneous group that includes a wide variety of plastic types including polycarbonates, polyamides such as nylon, acrylics, acrylonitrile butadiene styrene (ABS), bioplastics such as polylactic acid (PLA) and multi-layered or mixed-material composites.

Table 1. Types of plastic, their resin identification codes (RICs), and chemical structures.

Resin Identification Code (RIC)	Type of Plastic	Chemical Structure	Uses
1 PET	Polyethylene terephthalate		Bottles for water, soda drinks, caps, jars, microwavable trays, fibres for clothing
2 HDPE	High-density polyethylene		Shampoo bottles, piping for water, detergent containers, boats
3 PVC	Polyvinyl chloride		Cleaning products, sheeting, window frames, plumbing products, electrical cable insulation
4 LDPE	Low-density polyethylene		Plastic films, shopping bags, plastic bags, clear food containers, disposable packaging
5 PP	Polypropylene		Yogurt cups, straws, hangers, automotive parts, medical devices, food containers
6 PS	Polystyrene		CD/ DVD cases, packing peanuts. Single-use disposable cutlery, trays
7 OTHER	Other	Polycarbonates, polyamides, bioplastics, mixed-material composites	--

1.3 Recycling Pathways for Plastic Waste

Plastic waste recycling can be classified into four main stages (summarised in Figure 2): primary recycling (re-extrusion) where uncontaminated plastic waste is made into the same product. Secondary recycling, often referred to as mechanical recycling[14], involves the physical reprocessing of the polymer, however, this method frequently results in degraded material properties. Tertiary recycling, or chemical recycling, uses chemical processes to depolymerise or convert plastic waste into monomers to commodity chemicals[15]. Finally, quaternary recycling, also known as energy recovery, involves the combustion of plastic waste to generate energy[16]. Biodegradation, which involves microbial or enzymatic action in the breakdown of plastic[17] is also a distinct pathway for plastic waste treatment. Each recycling strategy plays a distinct role in the management of plastic waste and vary significantly in terms of environmental impact, technological maturity, and circularity potential[18,19]. For example, while primary and secondary recycling methods are more established, they often suffer from quality loss and have limitations with mixed or contaminated plastic waste streams. Quaternary recycling, while effective at reducing waste volume, is the least circular due to the destruction of material value and production of greenhouse gases (GHGs) due to incineration[9]. Tertiary recycling, or chemical recycling offers greater flexibility and potential for high-quality output, though it is less technologically mature and more energy intensive. This thesis focuses on chemical recycling and therefore, the other strategies will not be discussed further.

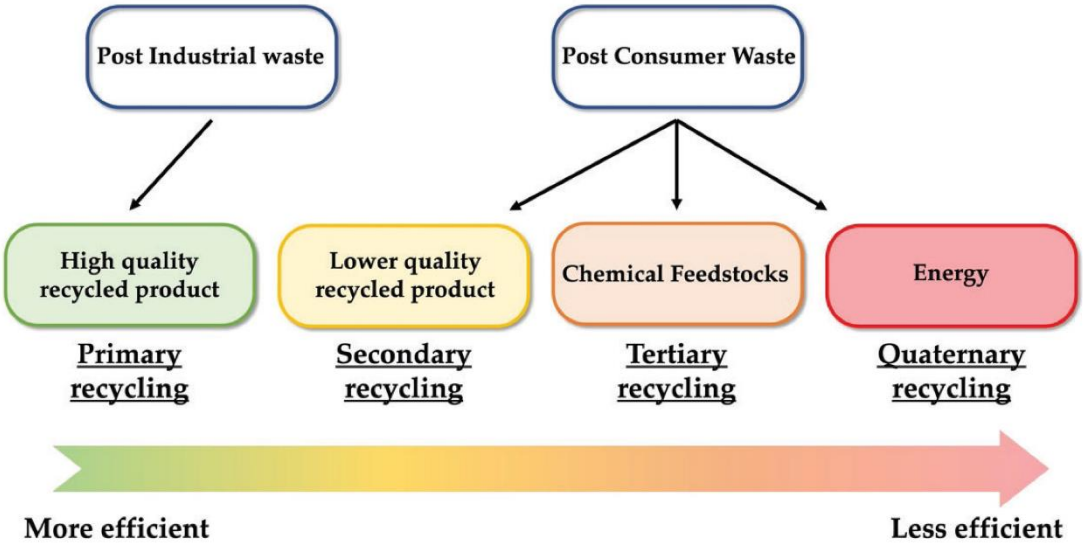


Figure 2. Common classification of usual recycling strategies for plastic wastes. Figure has been reproduced from ref[20].

Existing strategies for managing plastic waste are not sufficient to effectively mitigate the ongoing rise in plastic waste accumulation. Among emerging alternatives, chemical recycling, or feedstock recycling, offers a promising approach by converting waste plastics into valuable chemical feedstocks[21–23]. Chemical deconstruction has significant potential to enable closed-loop recycling systems for plastic waste thereby supporting a more circular economy[24,25]. The most common pathway for plastics at the end of their life is thermolysis, a chemical recycling process using elevated temperatures to break down polymers into smaller molecules which can be further sub-divided into three main categories: pyrolysis, hydrogenation, and gasification. To enhance the efficiency and selectivity of these processes, catalytic techniques such as hydrocracking and catalytic depolymerisation have been developed. These catalytic methods offer advantages including reduced reaction temperature, improved product yield as well as enhanced selectivity toward desired chemicals[26]. Pyrolysis is a more common thermochemical process where plastic waste undergoes

thermal or catalytic decomposition in the absence of oxygen to produce smaller molecules[27]. In contrast, gasification involves partial oxidation of plastic waste using a gasifying agent for example steam, oxygen or air[28]. This process produces synthesis gas (syngas) which is a mixture of hydrogen (H_2) and carbon monoxide (CO), along with byproducts such as carbon dioxide (CO_2) and methane (CH_4). Another area of increasing interest is chemical recycling to monomer (CRM)[29], a depolymerisation-based approach that breaks down plastic waste into their constituent monomeric units, which can subsequently be purified and then repolymerised to give recycled plastics with comparable performance to virgin resins[30].

Among the commonly used plastics PE, particularly in its low-density form (LDPE), has played a significant role in the proliferation of single-use plastics, due to its lightweight, flexible, and cost-effective nature. LDPE is a semi-rigid polyolefin, characterised by a branched molecular structure including both short and long branches along its backbone. These structural features give LDPE many desirable properties such as chemical resistance, transparency, and ease of processing, making it widely used in disposable packaging, grocery bags, squeeze bottles, medical supplies, and agricultural films. While LDPE stands out as one of the most widely produced and used polymers, it has one of the lowest recycling rates among the major plastic types. This is largely due its high contamination levels in waste streams coupled with its poor compatibility for mechanical recycling[31].

1.4 Post-Consumer Plastic and Plastic Additives

While many literature studies look at relatively simple polymer systems or pure polymer resins, real world post-consumer plastics are significantly more complex. Plastics are composed of a base polymer matrix combined with a complex blend of chemical additives, which are essential for modifying the performance, processability, and appearance of the final product. From the beginning of the plastic era in the 19th century, additives have played a crucial role in the development of polymeric materials. For example, the first commercial thermoplastic—celluloid, incorporated powdered camphor as a plasticiser to provide flexibility[32]. Additives are indispensable in polymer formulations, providing enhancements such as increased durability, UV resistance, flexibility, and visual appeal. Additives fall into four primary categories: (1) Functional additives which improve processing or application performance e.g. plasticisers and flame retardants, (2) Colourants such as dyes and pigments that provide aesthetic colouration and product differentiation, (3) Filler substances like calcium carbonate, mica and talc that lower costs and may enhance mechanical properties, and (4) Reinforcements which are materials such as glass or carbon fibres that improve strength and stiffness[33].

Plasticisers are low-molecular weight liquids—usually phthalate esters—that intercalate between polymer chains, improving their processability, flexibility and softness by lowering the glass transition temperature (T_g) of the polymer[34]. Plasticisers are typically incorporated into PVC, totally changing its mechanical properties and is used to make a variety of products including medical tubing, blood bags, and shower curtains. Fire retardants are used to control ignitability and flame propagation in the final product and are classified into primary and secondary flame

retardants. Primary flame retardants (brominated flame retardants) provide a commercially viable level of fire resistance on its own, whereas a secondary flame retardant or synergist (antimony trioxide), has little resistance on its own but can substantially enhance the performance of a primary flame retardant when coupled together[33]. Stabilisers make up a class of additives used to preserve the physical and chemical integrity of the polymer in the presence of oxygen, mechanical shear, thermal, photochemical, and environmental factors. There are several types of stabilisers for example, antioxidants—such as hindered phenols and aromatic amines—prevent oxidative degradation through free-radical scavenging and decomposition of hydroperoxides[35,36]. Photostabilisers (UV stabilisers/ UV absorbers (UVAs)) like benzotriazoles, hindered amine light stabilisers (HALS) and carbon black have radical scavenging abilities which protect against photooxidation. Heat stabilisers typically categorised as primary and secondary, prevent thermal degradation of polymers, in particular PVC, when exposed to elevated temperatures. For PVC, primary heat stabilisers function by scavenging HCl and eliminating defect structures. They are based on mixed metal salts (calcium/zinc), organotin compounds and metal-free organic-based systems[37]. Secondary heat stabilisers such as phosphites and thioesters, act as synergists by decomposing peroxides into stable non-radical products[38]. Lastly, metals such as copper, iron or nickel (prooxidants) can be introduced into the polymer through other additives, accelerating oxidative degradation of the polymer. Metal deactivators prevent this metal-catalysed oxidation by chelating with the metals and therefore, decreasing their catalytic activity. Colourants are widely used in plastic manufacturing to achieve specific aesthetic appearances. There are inorganic pigments—which scatter and absorb

light—and are generally insoluble in polymers and there are organic dyes which are soluble in the polymer and only absorb light[34]. Beyond the conventional additive classifications, compatibilisers have become increasingly important, particularly in blends of immiscible polymers. Compatibilisers are designed to have structural characteristics of both polymers being blended, as a result, many of these compounds are block or graft copolymers. For example, a PE-PS compatibiliser is used to blend PE and PS. These additives reduce the interfacial tension to facilitate uniform dispersion of the polymers while also increasing the adhesion properties of the polymers thereby improving the mechanical properties in polymer blends[39].

Most additives are not chemically bound to plastics and can therefore leach into ecosystems and foodstuffs posing a significant challenge to plastic circularity and raise concerns regarding human and environmental health impacts[40,41]. Different plastics have different applications and properties and hence are utilised in different ways as required by the material's quality or product design. Below is Table 2 summarising the common types of additives used in plastic manufacturing.

Table 2. Common types of additives used in the manufacture of plastics, examples[3,33,35,42–45], and their function in plastics.

Additive Type	Typical Loading (%)[34,42]	Function in Plastic	Polymer Types Used In
Fillers	10-50	Reinforcement/reduction of costs	PVC, polyesters
Common Examples:	Glass fibre, calcium carbonate, chalk, talc, clays, silica, asbestos, ceramic, porcelain clay, wood powder		
Plasticisers	20-50	Lower melt viscosity, improve processibility, flexibility, softness by reducing glass transition temperature	PVC, cellulose
Common Examples:	**Phthalates**: Dioctylphthalate (DOP), Di(2-ethyl hexyl) phthalate (DEHP), Diisononyl phthalate (DINP), Di n-butyl phthalate (DBP), Butyl benzyl phthalate (BBP) **Non-phthalate:** phosphoric esters, adipates, benzoate esters		
Flame Retardants	10-20	Reduce flammability	PVC, PC, ABS, EPS, HIPS, PE, PP
Common Examples:	**Primary:** Aluminium hydroxide, ammonium phosphates (APP), expandable graphite (EG), aluminium diethylphosphinate (DEPAL), tetrabromobisphenol A (TBBPA) **Secondary:** antimony trioxide (Sb_2O_3), zinc borate, montmorillonite (clay)		
Stabilisers	0.1-10	UV-, thermal-, photo-stabilisers for better durability and prevent degradation	PVC, PC, polyolefins, PS, cellulosic polymers, polyamide
Common Examples:	**Heat stabilisers: primary -** mixed metal salt blends, organotin compounds, lead compounds; **secondary -** alkyl organophosphites, epoxy compounds, beta diketones **UV absorbers**: salicylates, phenyl ketones, benzotriazoles, triazines, hindered amine light stabilisers (HALS), carbon black **Antioxidants**—butylated hydroxytoluene (BHT), hindered phenols, aromatic amines, phosphites, thioesters **Metal deactivators**—hydrazides, triazoles		
Compatibilisers	0.1-10	Improve compatibility in polymer blends	Mixed plastics
Common Examples:	Depends on the polymer to be blended **PE/PS**: PE-PS block copolymer **PE/PET**: SEBS styrene-butadiene-styrene triblock copolymer **PE/polyamide**: maleic anhydride (MAH)-grafted PE or PP		
Processing aids	0.5-2	**Lubricants**: Improve processing-lowering melt viscosity or reducing adhesion of plastic melt to metal surface **Mold release agents:** reduce sticking of the unfinished molding in the mold	Polyolefins, PVC, polyesters, bio-based (PLA & PHA)

		Emulsifiers: stability during processing **Antiblocking (slip) agents**: keep film from sticking during processing **Antifog agents**: reduce fogging by water vapour	
Common Examples:	**Lubricants**—Ca, Zn, Pb stearates, petroleum, fatty esters, amides. **Mold release agents**: waxes, silicones, fluorocarbons (powdered polytetrafluoroethylene dispersions), metal stearates, powdered polyethylene, mica, talc **Emulsifiers**: anionic, non-ionic, and cationic **Antiblocking (slip) agents**: fatty esters, waxes, metal soaps, polyamides (erucamide, oleamide, stearamide), silicones, polyethylene, poly-(vinyl alcohol), fluorocarbon polymers, inorganic silicates, silica **Antifog agents:** modified fatty esters, (poly) glycerol esters, alcohol ethoxylates		
Colourants	1-4	**Dyestuff**: soluble in the polymer to give transparent colour **Pigments**: insoluble and dispersed in plastic to adsorb and scatter light	Most/ all plastics
Common Examples:	**Dyes:** azocolourants, anthraquinone, phthalocyanine, quinacridone, isoindolinone **Pigments:** Titanium dioxide, zinc oxide (white); spinel black, iron oxide black (black); chrome iron brown, rutil brown (brown); iron oxide red, cadmium orange (red); chrome oxide green, cobalt spinel green (green); cobalt blue, ultramarine (blue); aluminium, copper (metallic)		
Others (antistatics, biocides, antiozonates, odorants)	1-2	**Antistats**: reduce static build-up, sparking, accumulation of dust. **Biocides**: prevent attack on plastic properties (Mold & fungus feeding on monomeric ingredients such as plasticisers)	Polyolefins (PE/PP), ABS, PVC, PS
Common Examples:	**Antistats**: fatty acid esters, alkyl sulfonates, phosphoric acid alkyl esters, quaternary ammonium compounds. **Biocides**: copper quinolinate, trichloromethyl phthalimide, quaternary ammonium compounds.		

Although additives play a crucial role in enhancing the performance of plastics such as improving processibility, safety, cost-efficiency, and durability, they also pose significant challenges during recycling processes, particularly in mixed-plastic waste streams where certain additives can impair processing. For example, abrasive additives such as fillers can interfere with near-infrared (NIR) sorting technologies preventing accurate polymer identification[46]. There is also the added risk that additives can transfer into new products during recycling or release into the environment, where they can leach into ecosystems, posing risks to both human health and biodiversity[47–49]. The compositional diversity of post-consumer plastic waste, which often includes incompatible polymer blends rather than well-defined single-polymer streams further complicates recycling and can result in inferior mechanical properties in recycled products, resulting in downcycling[50]. The vast number of additives used in commercial plastics contributes to the complexity of plastic waste streams, often making the recycling process technically and environmentally unfeasible[41].

This study focuses on the thermo-oxidative degradation of LDPE, as a chemical recycling strategy with a comparative analysis between pristine LDPE resin and post-consumer LDPE (PC-LDPE) waste. The recycling of post-consumer plastics is of paramount importance as land filling and incineration becomes more expensive and environmentally risky, however, the shift toward plastic sustainability is a complex and systemic challenge—one that cannot be resolved by recycling alone.

Despite growing interest in chemical recycling technologies, comparative studies between post-consumer and pristine LDPE are scarce in literature. PC-LDPE presents additional challenges such as the presence of additives within the polymer matrix,

potentially affecting chemical reactivity and efficiency of the degradation process, limiting our understanding of how real-world plastic waste behaves in chemical degradation systems. The introduction chapter presents a general overview of plastic waste recycling technologies, in particular chemical recycling, and the challenges associated with it. The aim of this thesis is to investigate the catalytic thermo-oxidative degradation of LDPE with focus on comparing the degradation behaviour of post-consumer waste with commercial virgin resin.

Chapter 2
Experimental

Chapter 2:

2.1 Introduction

Materials and products investigated in this study were characterised using a combination of analytical techniques, including Fourier-transform infrared (FTIR) spectroscopy and X-ray photoelectron spectroscopy (XPS) to examine surface functionalities, as well as high-performance liquid chromatography (HPLC) to identify molecular degradation products. These complementary techniques enabled a comprehensive analysis of chemical structure, surface chemistry, and degradation pathways.

2.2 Fourier-transform infrared (FTIR) spectroscopy

Fourier-transform infrared (FTIR) spectroscopy is a surface-sensitive analytical technique, capable of probing only a few microns into the sample. It provides structural information based on the interaction of infrared (IR) light with molecular vibrations. In this study, the attenuated total reflectance (ATR) mode was employed, where the IR beam is directed into a high refractive index crystal (commonly diamond or germanium), resulting in total internal reflection. At each reflection within the ATR crystal, an evanescent wave penetrates a few microns into the sample. Specific molecular structures absorb characteristic frequencies of the IR radiation, while unabsorbed light continues to reflect within the crystal and is ultimately detected, generating a spectrum typically between 4000 cm^{-1} and 400 cm^{-1} range (Figure 3).

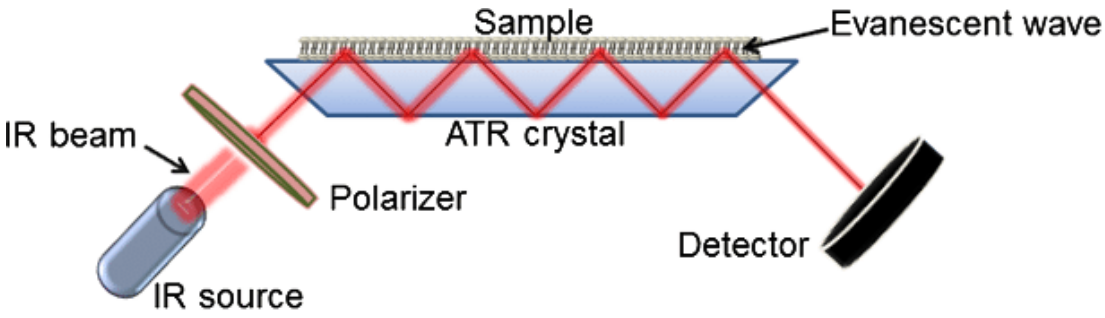


Figure 3. Schematic representation of an ATR-FTIR system reproduced from ref[51].

ATR-FTIR is especially valuable for the characterisation of polymeric materials, due to its ease of use, cost-effectiveness, sensitivity and minimal sample preparation requirements. In this work, IR spectra were obtained using a Nicolet 6700 (Thermo Fisher Scientific) equipped with a zinc selenide (ZnSe) ATR crystal, using Omnic 8.1 software. Data were derived based on 100 scans, resolution 4 cm^{-1}, using a KBr beamsplitter and DTGS thermal detector. Atmospheric correction was applied to remove contributions from ambient water vapour and CO_2.

FTIR spectroscopy enables monitoring of specific functional groups, such as the carbonyl (C=O) band, which serve as indicators of oxidative degradation. The carbonyl index (CI) is a widely used parameter for quantifying the extent of oxidative degradation and is calculated according to equation 1. The CI is calculated based on the relative intensity or integrated peak area of the carbonyl absorption band in the range of 1850 cm^{-1} - 1650 cm^{-1}, normalised to a reference peak that is considered stable and is unaffected by the degradation process. For this work, the integrated area was used for the calculation of the CI and the reference band was taken to be the CH_2 absorption peak at 1470 cm^{-1}.

$$\text{Carbonyl Index (CI)} = \frac{Area\ under\ carbonyl\ band\ 1850{-}1650\ cm^{-1}}{Area\ under\ reference\ band\ 1470\ cm^{-1}} \quad (1)$$

2.3 X-ray photoelectron spectroscopy (XPS)

X-ray photoelectron spectroscopy is a surface sensitive analytical technique that provides both quantitative and qualitative information about the elemental composition, chemical states and electronic environment of materials. It is capable of analysing the top few nanometres of a sample surface, making it particularly valuable for surface chemistry studies. In XPS, a sample is irradiated with X-rays usually aluminium Kα (Al Kα) or magnesium Kα (Mg Kα) which are absorbed by core-level electrons. If the energy of the incident X-ray photons exceeds the binding energy of these electrons, they are ejected from the atom via the photoelectric effect as illustrated in Figure 4. The kinetic energy (KE) of the emitted photoelectrons is measured by the spectrometer allowing the binding energies to be calculated according to equation 2, which are characteristic of specific elements and their chemical states.

$$E_{binding} = E_{photon} - (E_{kinetic} + \phi) \quad (2)$$

Where, $E_{binding}$ is the energy of an electron attracted to a nucleus; E_{photon} is the energy of the incident X-ray photons, $E_{kinetic}$ is the kinetic energy of the ejected electron and ϕ is the work function of the spectrometer.

XPS spectra are typically calibrated using a C 1s reference peak at 284.8 eV. Initially, a survey spectrum is collected from 0-1400 eV which detects all elements that are present in the sample. Subsequently, high-resolution scans are performed on the core levels of specific elements of interest within the sample to determine their oxidation states and chemical environments, as indicated by characteristic chemical shifts in the binding energies. The resulting spectrum is a plot of electron count versus

binding energy and the area under each peak corresponds to the relative number of atoms of that element. For electrons occupying p, d, and f orbitals, spin-orbit coupling can lead to peak splitting, giving rise to the appearance of doublets. This splitting arises from the interaction between an electron's intrinsic spin and its orbital angular momentum, causing slight differences in binding energy resulting in two distinct but closely spaced energy levels.

In this study, XPS analysis was carried out using a KRATOS ACIS 165 monochromatised X-ray photoelectron spectrometer equipped with an Al Kα (hv = 1486.6 eV) X-ray source. Spectra were collected at a take-off angle of 90° and all spectra were referenced to the C 1s peak at 284.8 eV.

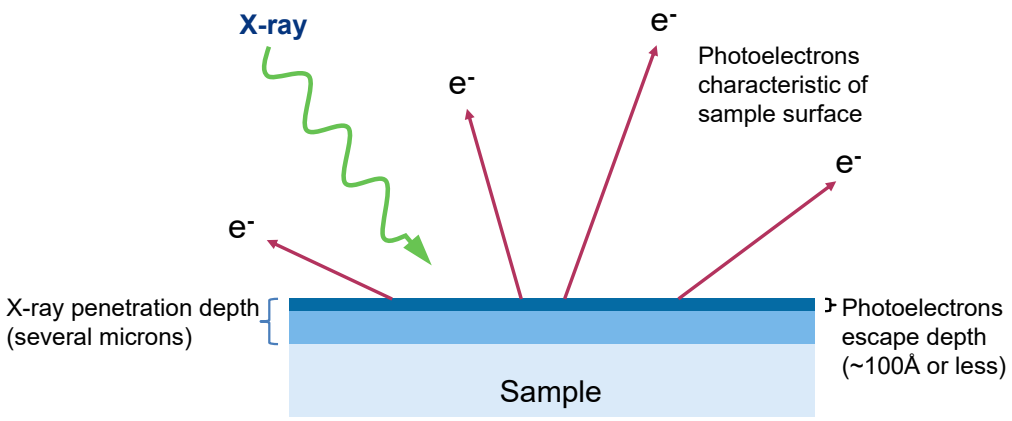


Figure 4. Schematic representation of the XPS process reproduced from ref[52].

2.4 High performance liquid chromatography (HPLC)

High performance liquid chromatography (HPLC) is a highly sensitive analytical technique used to separate, identify and quantify semi-volatile and non-volatile compounds in liquid samples. The separation relies on the pressure-driven movement of a mobile phase through a column containing a stationary phase. The column used throughout this work was an Agilent Hi-Plex H (300 x 7.7 mm) size

exclusion column, operating under ion-exchange and size exclusion principles with specific applications for carbohydrates, sugars and organic acid analysis. As illustrated in Figure 5, this column is packed with sulfonated polystyrene divinylbenzene resin with controlled pore sizes, allowing for selective interactions, which are dependent on the differing affinities of the analyte for the stationary phase column, to occur. The typical mobile phase for this column is dilute sulfuric acid (H_2SO_4), protonating the column and thus, facilitating ion exchange effects. In this work, HPLC was used to separate and identify the acid products formed from the thermo-oxidative treatment of LDPE. Samples were analysed using an Agilent 1200 HPLC coupled to a UV detector (210 nm). Samples were prepared by mixing 500 µL of the product solution generated from the thermo-oxidative degradation of low-density polyethylene (LDPE) with 500 µL of the mobile phase, giving a dilution factor of 2. The mobile phase was 2.5 mM H_2SO_4 with a constant flow rate of 0.5 mL min^{-1} and the column was maintained at a constant temperature of 50 ^oC, following the method and column specifications of Bäckström *et al.*[53]. Quantitative analysis was performed by comparing peak areas of the analytes with external calibration curves, that were previously prepared using standard solutions of known concentrations of various carboxylic acids including: succinic, formic, glutaric, acetic, adipic, propionic, butyric and pimelic acid.

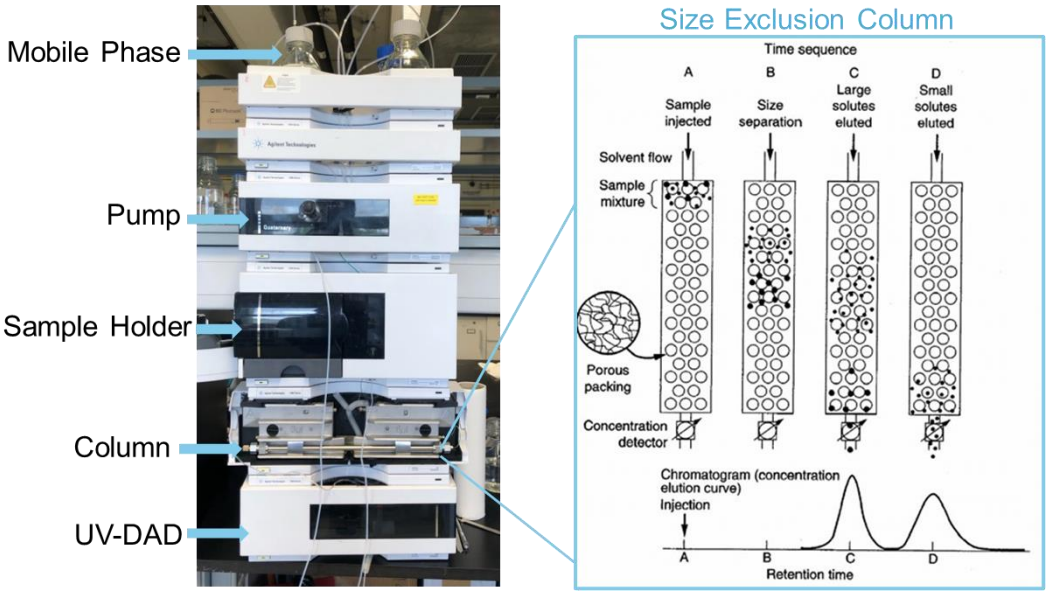


Figure 5. HPLC setup used and schematic for the mechanism of size exclusion column reproduced from ref[54].

2.5 Thermo-Oxidative Reactions: Carousel 12 Plus Reaction Setup™

All thermo-oxidative reactions were carried out in a Carousel 12 Plus Reaction Station™ shown in Figure 6 (a). Each reaction was carried out in borosilicate glass tubes into which the plastic substrate, catalyst, radical initiator, and solvent were introduced. The tubes were then sealed using PTFE caps, also depicted in Figure 6 (b). During the reaction, the valve is closed, and the silicon septum enabled the instantaneous release of overpressure, ensuring safe and stable conditions throughout the thermal treatment. Once the reaction is complete within the specified timeframe, the polyethylene samples are collected by suction filtration, washed with deionised water (DI) and dried overnight in an oven.

Thermal degradation of LDPE was carried out under ambient air at a temperature of 120 °C and a stirring speed of 800 RPM. A 30 min ramp time was required to reach

the target temperature, after which the reaction was maintained at 120 °C for varying durations depending on the specific reaction conditions.

The extent of plastic degradation was assessed by calculating the plastic mass loss according to equation 3:

$$\text{Mass loss of plastic} = \frac{W0 - W1}{W0} \text{ x } 100 \quad (3)$$

Where W_0 is the initial weight of plastic, and W_1 is the weight the plastic remaining post-reaction.

The approximate amount of oxygen available in the sealed reaction tubes was estimated using the ideal gas law. For a 50 mL tube containing 10 mL reaction solution (40 mL headspace), headspace oxygen corresponds to 0.26 mmol at 120 °C (assuming 21 % oxygen in air).

A key set of reactions using V-LDPE and PC-LDPE (120 °C, 5 h, Mn-Fe catalyst, NHPI, acetic acid) were used as a reference to determine the experimental variability. For V-LDPE, the reference reaction gave a mean mass loss 6 ± 10 %, n=3 (the relatively high standard deviation can be attributed to variability in the physical behaviour of the samples during the reaction; congealing ≈ 0 %, no congealing ≈ 17 %), while the mean mass loss for PC-LDPE was 30.9 $\pm$ 2 %, n=3.

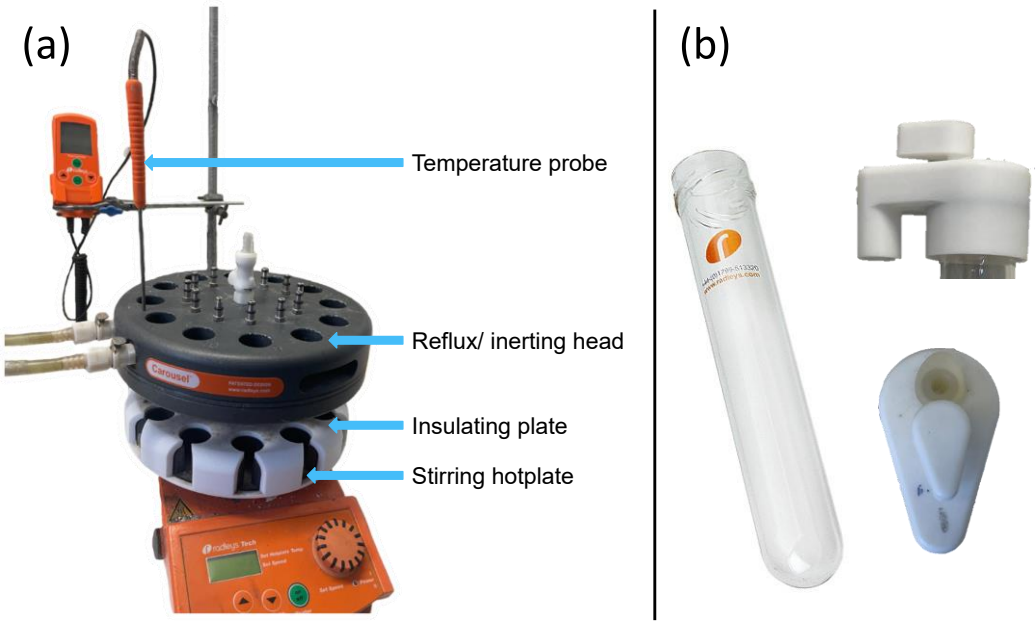


Figure 6. (a) Carousel 12 Plus Reaction Station™ setup with (b) glass tube and PTFE cap.

2.6 Catalyst Preparation

All catalyst syntheses were performed by another member of the research group. Consequently, characterisation results such as X-ray diffraction (XRD) and BET surface area analyses are not presented in this thesis.

2.6.1 Homogeneous catalyst

The homogeneous catalysts cobalt(II) acetate tetrahydrate ($Co(OAc)_2.4H_2O$) and manganese(II) acetate tetrahydrate ($Mn(OAc)_2.4H_2O$) were purchased from Sigma-Aldrich and used as received without further treatment.

2.6.2 Fe_2O_3 (hematite)

The hematite catalyst (Fe_2O_3) was synthesised by simple co-precipitation method following the procedure of Farahmandjou *et al.*[55]. $FeCl_3.4H_2O$ (2 g) was dissolved in

DI water (50 mL) and stirred at room temperature (rt) for 10 min. the pH was adjusted to pH 12 using 1M NaOH solution. Once a rusty brown precipitate had formed, the mixture was stirred under reflux for 2 h at 100 °C under N_2. The solid Fe_2O_3 particles were then collected by suction filtration and dried in an oven at 75 °C overnight. Finally, the resulting solid was calcined at 450 °C for 4h.

2.6.3 Fe-CeO_2 catalyst

The solid solution Fe-CeO_2 catalyst was prepared following the method of Breen et al.[56]. A solution of $FeCl_3.4H_2O$ (0.378 g) in 25 mL DI H_2O and $Ce(SO_4)_2.4H_2O$ (1.933 g, 0.2 M) in 25 mL DI H_2O were combined to form a 1:2 molar ratio of Fe:Ce and stirred at rt for 10 min. The pH was adjusted to pH 12 using 1 M NaOH resulting in a red/brown precipitate. The mixture was stirred under reflux for 2 h at 100 °C under N_2. The resulting particles were collected by suction filtration and dried in an oven overnight at 75 °C. the solid was calcined at 450 °C under air for 4 h. (See Figure 8 for SEM and EDX of the catalyst).

2.6.4 $MnFe_2O_4$ catalyst

The $MnFe_2O_4$ spinel catalyst was prepared by co-precipitation method following the procedure described by Wu *et al.*[57]. $Fe(NO_3)_3.9H_2O$ (4.04 g) and $Mn(NO_3)_2.4H_2O$ (1.26 g) were dissolved in 50 mL DI H_2O. The pH was raised to pH 12 using 10 % NaOH solution and left to stir for 30 min. the suspension was heated to 100 °C and refluxed for 2 h. The solid was collected by suction filtration and left to dry in an oven at 75 °C

overnight. The solid was then placed in an oven at 110 °C for 3 h and annealed at 600 °C for 1 h. (See Figure 9 for SEM and EDX of the catalyst).

2.6.5 $CoFe_2O_4$ catalyst

The $CoFe_2O_4$ spinel catalyst was prepared using the same method as above with $Fe(NO_3)_3.9H_2O$ (4.04 g) and $Co(NO_3)_2.6H_2O$ (1.46 g) annealed at 600°C for 1 h.

Chapter 3

Results & Discussion

Chapter 3:

3.1 Introduction

3.1.1 Research Aims and Objectives

This chapter presents and discusses the experimental results obtained during the thermo-oxidative degradation of low-density polyethylene (LDPE), both virgin resin and post-consumer packaging waste. Techniques including Fourier Transform Infrared Spectroscopy (FTIR) and X-ray Photoelectron Spectroscopy (XPS), were employed to characterise the structural and chemical changes occurring in the LDPE samples under various conditions. High-Performance Liquid Chromatography (HPLC) was used to identify the products formed in the oxidation reaction.

The oxidative-degradation methodology used in this work builds on a catalytic oxidation protocol reported in a recent Science article reported by Sullivan *et al.*[22] who demonstrated the conversion of diverse polymeric feedstocks into a mixture of oxygenated small molecules using a homogeneous catalyst system that represent useful substrates for subsequent bioconversion. The initial catalytic step uses metal-promoted autoxidation to depolymerise mixed plastics into oxygenated intermediates in an acetic acid solvent. The catalyst used were homogeneous cobalt and manganese salts in the presence of an initiator, N-Hydroxyphthalimide (NHPI). The Co/Mn/NHPI-promoted autoxidation in acetic acid converts diverse plastics, including polyethylene, into oxygenated, water-soluble products between 160–210 °C under high pressure conditions (8 bar O_2, 72 bar N_2). Their study also showed that post-consumer substrates perform similarly to commercial resins under

identical conditions. In light of these considerations, this thesis was undertaken to address the following research aims:

Aim 1: Explore a heterogeneous catalyst analogue in acetic acid.

Where the original study utilised homogeneous catalytic systems, this research investigates whether a heterogeneous catalyst can replicate the Co/Mn/NHPI autoxidation reactivity in acetic acid, generating the PINO-derived hydrogen-abstraction pathway while enabling catalyst separation and reuse. This aim translates the homogeneous conditions of Sullivan *et al.* into a greener, operations-friendly format that minimises metal contamination.

Aim 2: Replace high pressure O_2/N_2 with ambient air.

This works evaluates whether air can be a substitute for O_2/N_2 (10/90 mixture) in the acetic-acid/Co–Mn/NHPI autoxidation of LDPE to enable oxidation to form mono and dicarboxylic acids. This approach is informed by previous work within the group utilising Fenton-type oxidations that operate effectively under ambient air conditions. Given the mechanistic similarities between these Fenton systems and the Co–Mn/NHPI process (both proceeding via radical-based pathways), it is hypothesised that air may provide sufficient oxidising capacity for effective polymer degradation.

Aim 3: Compare the degradation of virgin resin versus post-consumer LDPE in acetic acid.

This thesis directly compares the oxidative degradation behaviour of virgin LDPE resin versus LDPE derived from post-consumer packaging. By subjecting both materials to identical thermo-oxidative conditions the study aims to uncover how polymer feedstock source, additives, or physical form influence degradation kinetics, surface oxidation and formation of oxidation products such as mono and dicarboxylic acids. This is significant as a criticism of plastic depolymerisation studies is only using pure resin polymers, which do not accurately reflect the degradation behaviour of real post-consumer plastic.

Through these research aims, the thesis advances the understanding of green chemistry and potentially scalable catalyst systems for LDPE upcycling and delivers critical insight into the role of feedstock origin on degradation efficacy.

3.2 Method development

3.2.1 Development of Reaction Apparatus

The initial degradation experiments were carried out in a round bottom flask (100 mL) under reflux conditions using a sand bath in a heating mantle. However, this reaction setup presented several limitations:

- **Temperature limitation**: Under reflux, the reaction temperature is constrained by the boiling point of the solvent, in this case, 118 °C for acetic acid.

- **Poor thermal conductivity**: Heat transfer in the round-bottom flask/sand bath system was inefficient. The combined thermal resistance of the glassware, sand, and solid polymer substrate led to uneven heating, particularly for semi-crystalline LDPE powder, resulting in non-uniform degradation.
- **Difficult product recovery**: The softened LDPE adhered to the curved interior of the flask, complicating recovery and leading to sample loss for post-reaction analysis.

To overcome these issues, the apparatus was transitioned to a sealed pressure tube system with a Radleys Carousel™ reactor. This setup allowed reactions to proceed at 120 ^{o}C without solvent loss and offered more efficient heat transfer due to direct contact between the tube and heated aluminium block. The sealed system also allowed for adequate pressure build-up, potentially enhancing the rate of polymer degradation. Additionally, the geometry of the tube allowed for easier recovery of the material without significant mass loss. Overall, the pressure tube system provided safer, more consistent, and more efficient reaction conditions, particularly for catalyst screening studies. The reaction temperature was confirmed by direct measurement of the acetic acid during the reaction.

3.2.2 Initial catalyst screening

This study began with the use of homogenous cobalt(II) acetate, manganese(II) acetate salts and NHPI as a radical initiator, following previously reported methods

by Sullivan *et al.* which is based on their established role in the Amoco Mid-Century (MC) process for the catalytic oxidation of hydrocarbons to carboxylic acids[58]. It was proposed by Ishii *et al.*[59] that the reaction pathway is similar to that of a free radical autoxidation. The NHPI radical initiator is oxidised in situ to the phthalimide N-oxyl (PINO) active radical species capable of abstracting hydrogen from relatively weak C–H bonds which plays a central role in initiating the oxidative degradation of polyethylene. In this system, Co(II) acetate is first oxidised to Co(III) by O_2 and is facilitated by the presence of manganese salts[60]. The resulting Co(III)-O_2 species converts NHPI into the PINO radical. PINO abstracts hydrogen from the polyethylene backbone, generating carbon-centred radicals that undergo further oxidation, ultimately leading to chain scission and formation of low-molecular weight oxidation products such as mono- and dicarboxylic acids (Figure 7).

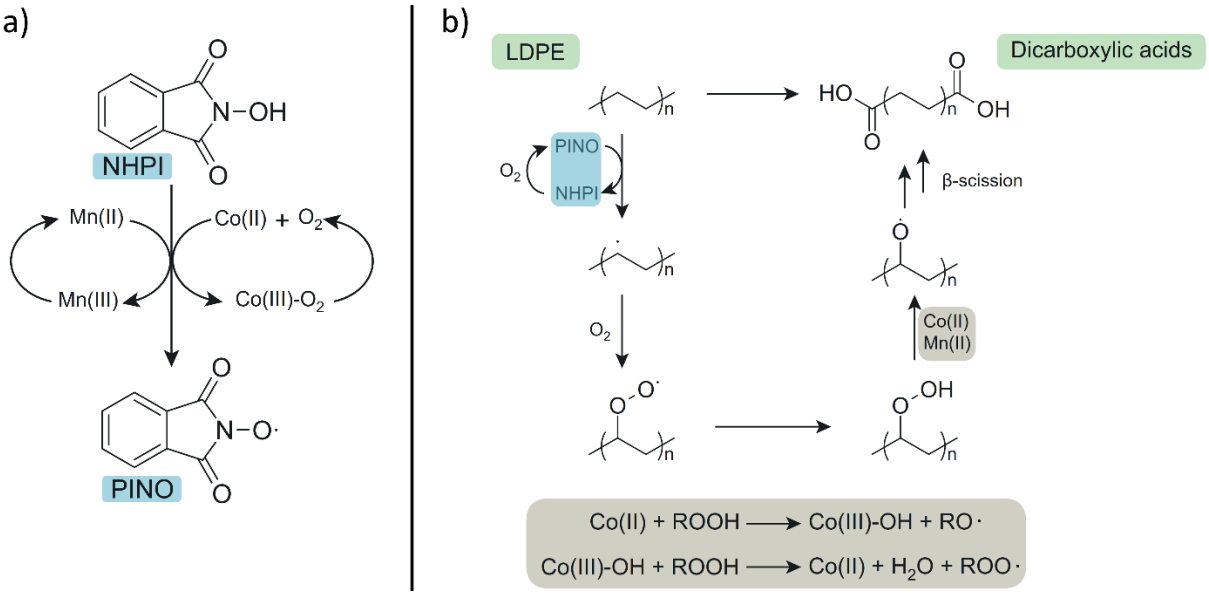


Figure 7. Schematic of the degradation mechanism. a) Conversion of NHPI to active species, PINO. b) Proposed pathway for the oxidative degradation of LDPE using NHPI and metal catalysts in the presence of O_2.

Acetic acid is used as a solvent throughout the study due to its availability, low cost and because MC catalysts exhibit increased activity in carboxylic acid media[61]. While homogeneous cobalt catalysts have been reported as effective catalysts for polyolefin depolymerisation[61–63], ethical and environmental concerns limit their desirability. Consequently, catalyst screening further expanded to include a series of heterogeneous systems on both virgin LDPE (V-LDPE) and post-consumer LDPE (PC-LDPE). The heterogeneous catalysts shortlisted here were prioritised because closely related Fe- and Fe-spinel formulations have shown excellent performance for Fenton-type oxidative degradation of LDPE under microwave irradiation. These reactions proceed via hydroperoxide decomposition to alkoxy radicals and promotion of chain scission. Although the present study employs conventional thermo-oxidative conditions in acetic acid, both are radical mediated mechanisms. The heterogeneous catalysts specifically used were haematite (Fe_2O_3), iron-ceria mixed solid solution (Fe-CeO_2), cobalt ferrite ($CoFe_2O_4$) and manganese ferrite ($MnFe_2O_4$) catalysts.

Initial catalyst screening was benchmarked by mass loss of the plastic to evaluate the potential for catalytic thermo-oxidative degradation of LDPE in acetic acid at 120 °C for initially 5 h (summarised in Table 3). Pure iron oxide was initially tested as a single metal catalyst and exhibited promising mass loss but was not ultimately selected for further study due to potential advantages of bimetallic systems, where synergistic effects between metals may enhance catalytic activity. Following this, a cobalt-iron (Co-Fe) catalyst was investigated which showed effective mass loss however, as mentioned previously, its ethical and supply chain concerns led to its exclusion in favour of a manganese-iron (Mn-Fe) mixed-metal catalyst. Manganese and iron are

both earth-abundant, low-toxicity metals, as well as this, the catalyst demonstrated comparable degradation performance to other systems. Heterogeneous catalysts by nature are also easily separated and recovered from the reaction mixture. Therefore, the Mn-Fe catalyst was selected for further study based on its catalytic activity, material sustainability and ethical considerations. Transitional metals are widely used as additives in polyolefins to promote oxidative degradation during UV or heat exposure, catalysing radical formation and chain scission. Their appeal stems from their ability to catalyse the breakdown of hydroperoxides into alkoxy radicals, which promote chain transfer reactions during the autoxidation of the polymer backbone. Figure 8 and Figure 9 shows SEM and EDX images of two tested catalysts: Fe-CeO_2—which has been reported in literature as effective oxidation catalysts for example in Fenton-type oxidation[56], additionally, this catalyst is the subject of on-going research within our group, and $MnFe_2O_4$—which was selected for further study.

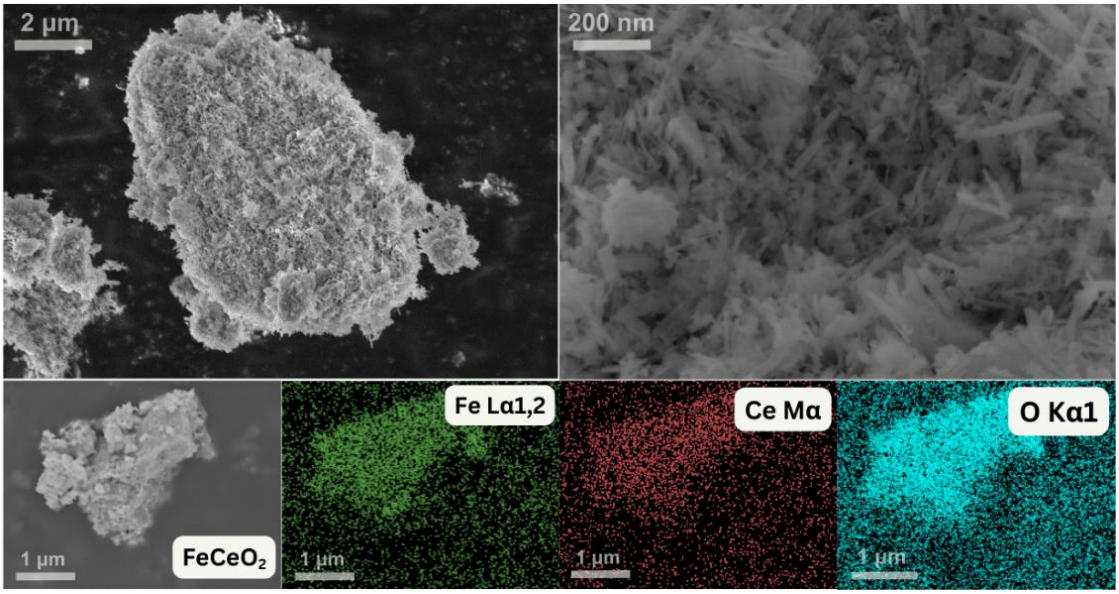


Figure 8. SEM micrograph and corresponding EDX of the Fe-CeO_2 catalyst. The SEM image reveals the surface morphology, while the EDX analysis confirms the presence of Fe, Ce and O distributed evenly within the material.

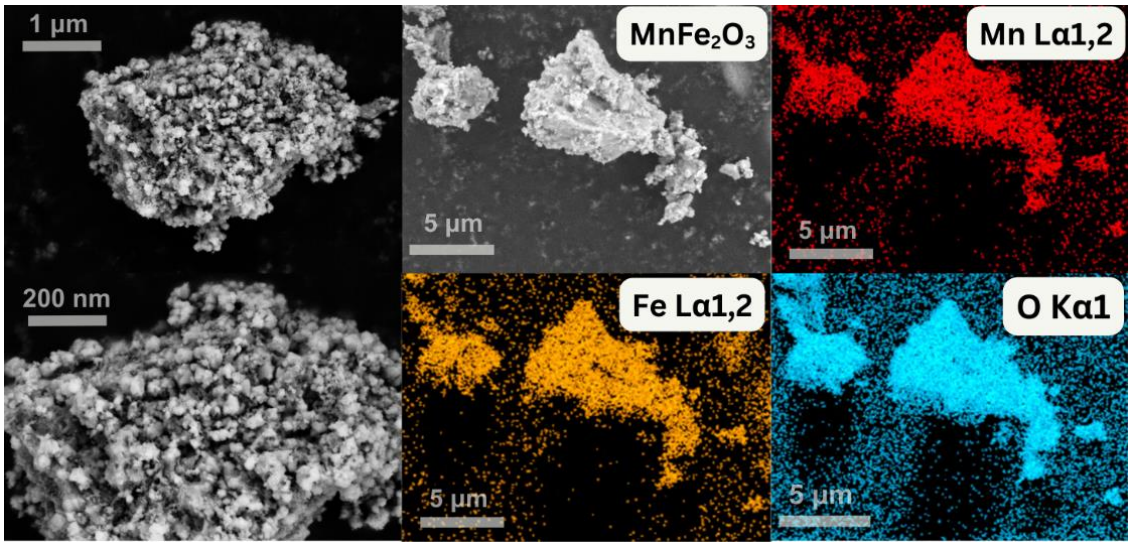


Figure 9. SEM micrograph and corresponding EDX of the Mn-Fe catalyst. The SEM image shows a heterogeneous surface morphology, while the EDX analysis confirms the presence of Mn, Fe and O evenly distributed within the material, consistent with the intended mixed- metal composition.

Table 3. Summary of catalysts used for LDPE degradation experiments (For catalyst synthesis, see Experimental section for further details).

Catalyst Composition	Preparation Method	V LDPE Mass loss (%)	PC-LDPE Mass loss (%)	Notes
Homogeneous Catalyst				
$Co(OAc)_2.4H_2O$/ $Mn(OAc)_2.4H_2O$	Commercially sourced	4	33	Based on Amoco MC autoxidation process, discontinued due to ethical & environmental concerns
Heterogeneous Catalysts				
Fe_2O_3	Synthesised	5	35	No potential for synergistic activity
Fe-CeO_2	Synthesised	4	31	Moderate performance
$CoFe_2O_4$	Synthesised	0	30	Discontinued due to ethical & environmental concerns
$MnFe_2O_4$	Synthesised	11	33	Selected for further study

Initially, samples were subjected to overnight stirring in acetic acid at room temperature as a pre-treatment to assess whether prolonged exposure might promote functionalisation of the surface of the polymer and therefore depolymerisation. Acid pre-treatment involving the stirring of polyethylene in strong mineral acids such as sulfuric and nitric acid, is well known to induce surface oxidation which is beneficial for further oxidative degradation of the polymer. However, pre-treatment by stirring in acetic acid produced negligible differences in mass loss as shown in Figure 10. Consequently, the pre-treatment was excluded from further experiments to streamline the process.

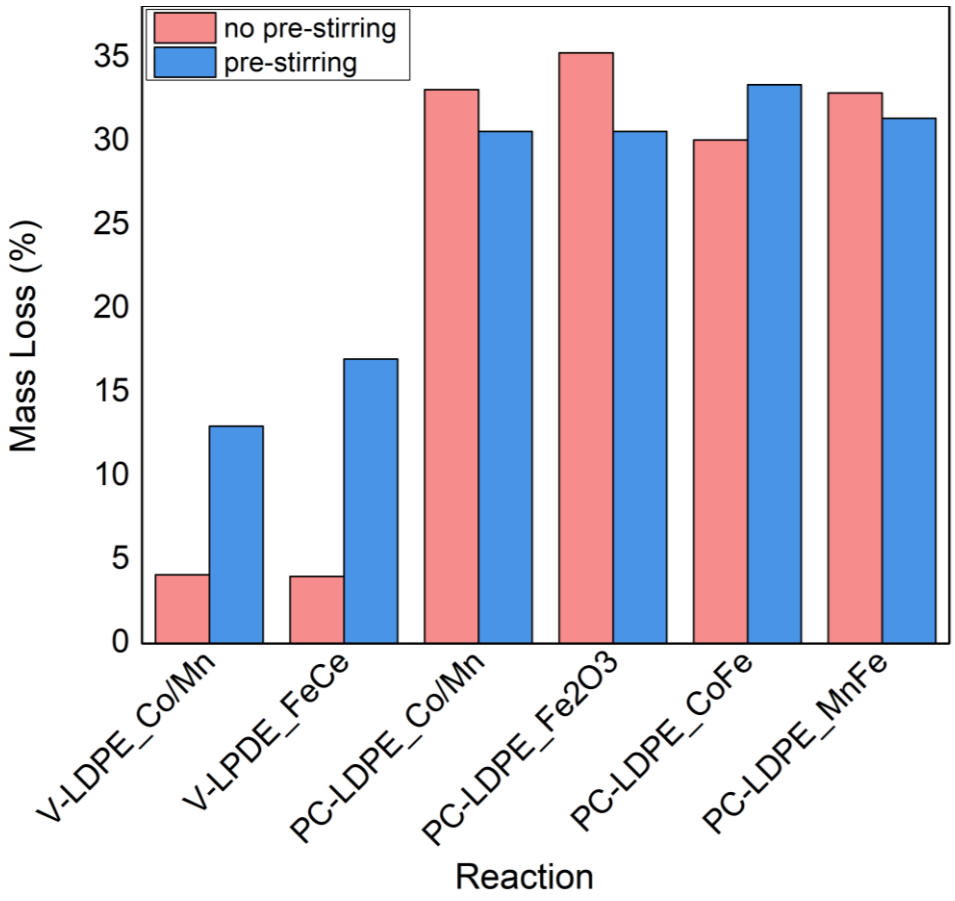


Figure 10. Effect of overnight stirring in acetic acid on LDPE mass loss for different catalytic systems. General variability in mass loss was obtained from a set of key reference reactions (see Experimental Section for further details). The mean mass loss for V-LDPE was 6 ± 10 %, n=3, while the mean mass loss for PC-LDPE was 30.9 ± 2 %, n=3.

3.2.3 Comparing the effects of oxidative thermal-catalytic treatment on pristine LDPE resin and post-consumer LDPE film

Preliminary screening identified a clear trend in the behaviour between virgin LDPE and post-consumer LDPE, with PC-LDPE having higher mass loss across all catalysts evaluated. Two complementary readouts were used: (1) mass loss, which provided a coarse measure of bulk degradation and (2) FTIR spectroscopy, to assess surface oxidation through the emergence of oxygen-containing functional groups and calculation of the carbonyl index (CI). The CI normalises the carbonyl peak to a stable methylene band, enabling comparisons across different samples (see Experimental Section for further details).

Across all catalysts, virgin LDPE showed minimal mass loss, typically in the range of 0-17 % indicating limited degradation under the applied conditions. A key physical effect may have dominated this outcome: it was observed that the LDPE powder congealed into a solid mass or 'ball' during the reaction (Figure 11). Congealing collapses surface area and restrict access of oxidant and catalyst, suppressing further reaction. In contrast, samples that remained dispersed (in powder form) under otherwise identical conditions exhibited greater mass loss reaching up to 17 %, underscoring the critical role of surface accessibility.

To probe the polymer morphology, experiments with large LDPE beads also gave low or negligible mass loss consistent with their reduced specific surface area. Removing the stir bar and relying on boiling-solvent agitation for 5 h produced the same congealing and no mass loss, indicating the effect is not primarily mixing-limited. Instead, it reflects intrinsic LDPE properties, in particular its low melting point (~110 °C) and semi-crystalline character, promoting sintering/fusion under the

reaction conditions. Collectively, these results are consistent with surface deactivation as formation of a fused mass that shields reactive sites and slows oxidation.

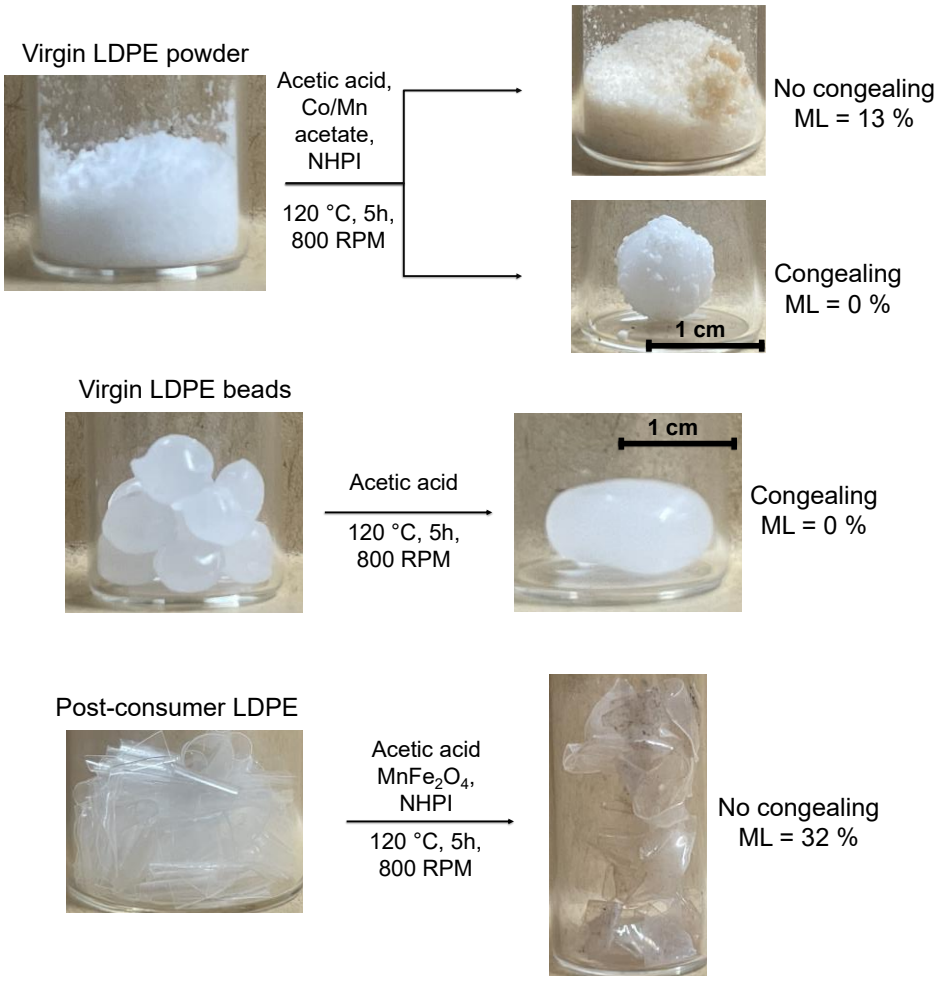


Figure 11. The effect of congealing on mass loss. Unlike PC-LDPE which does not congeal, when V-LDPE undergoes thermal treatment in the absence or presence of catalyst and NHPI, it will either congeal or remain dispersed in solution. However, once congealing occurs, the surface becomes deactivated and prevents further reaction.

FTIR analysis was used to investigate changes on the polymer surface of virgin and post-consumer LDPE following thermo-oxidative treatment by monitoring functional-group changes on the polymer surface before and after treatment. Pre-reaction

spectra for both V-LDPE and PC-LDPE show the characteristic LDPE bands as reported in literature[64]: bands at 717 cm^{-1}, corresponding to CH_2 rocking; 1367 cm^{-1} arising from the methyl group (CH_3); at 1461 and 1471 cm^{-1}, attributed to the symmetric and asymmetric of CH_2 bending respectively; and at 2846 and 2913 cm^{-1}, corresponding to the symmetric and asymmetric stretching of C-H bond of the CH_2 groups, respectively (Figure 12). After the reaction with the homogeneous Co/Mn acetate catalyst, no new bands were observed for V-LDPE, indicating no measurable surface functionalisation of virgin LDPE. However, when V-LDPE is reacted with a heterogeneous catalyst ($CoFe_2O_4$), under the same conditions a distinct carbonyl peak at 1718 cm^{-1}**,** indicating a degree of functionalisation as shown in Figure 13.

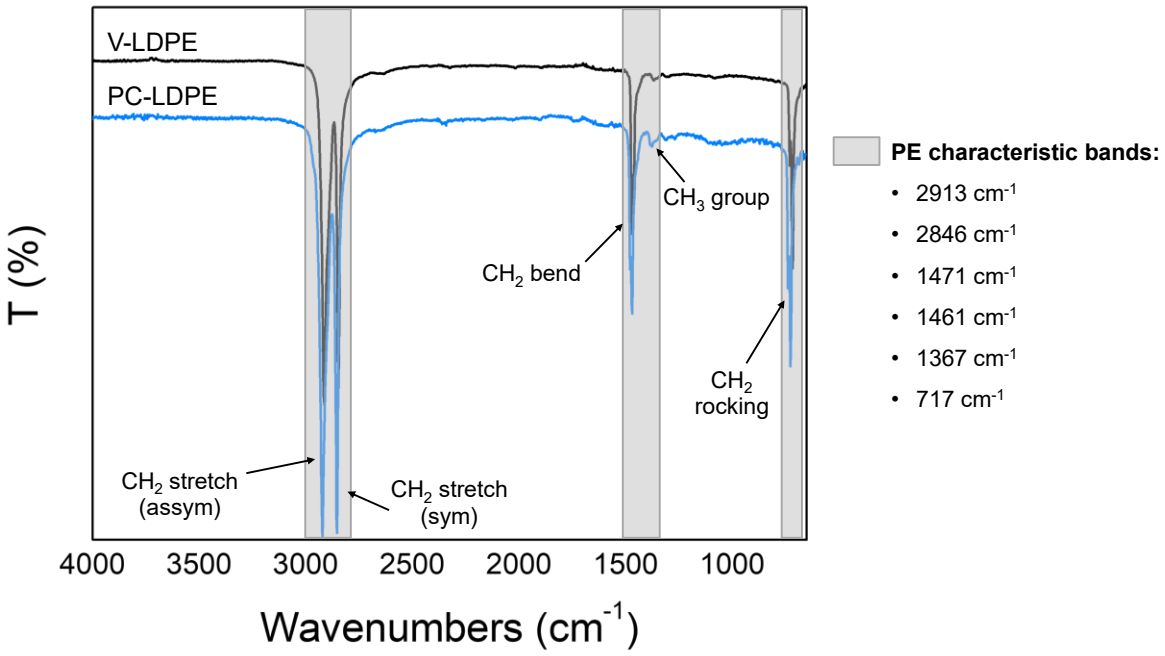


Figure 12. FTIR spectra of unreacted virgin LDPE (V-LDPE) and post-consumer LDPE (PC-LDPE) with characteristic PE bands.

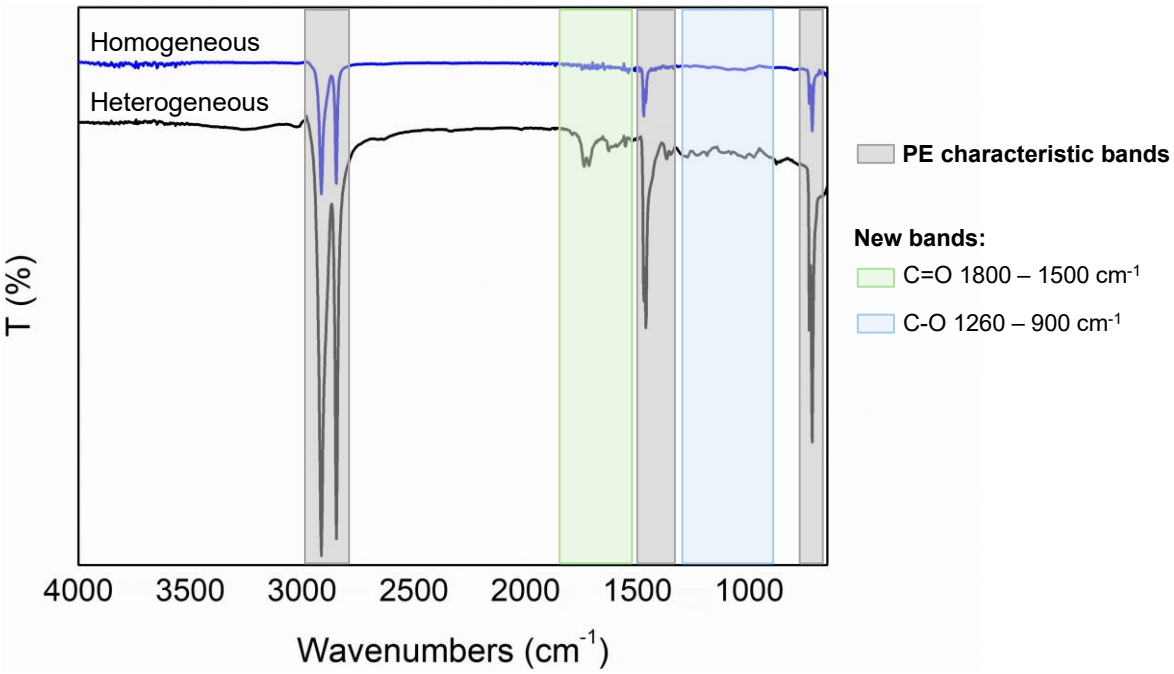


Figure 13. FTIR spectra of virgin LDPE after reaction with homogeneous (Co/ Mn acetate) and heterogeneous ($CoFe_2O_4$) catalysts. Sample treated with homogeneous catalyst (blue line) showed no functionalisation, whereas LDPE reacted with a heterogeneous catalyst (black line) exhibits clear peaks in the carbonyl region (1718 and 1627 cm^{-1}), along with weak bands in the C-O stretching region (1200-900 cm^{-1}), indicating oxidative functionalisation of the polymer.

As a contrast to the virgin LDPE, which showed minimal mass loss and congealing-limited reactivity, PC-LDPE was markedly more susceptibility to degradation, achieving ~30 % mass loss regardless of the catalyst employed. This suggests that the prior life cycle of PC-LDPE (additives, stabilisers, processing history) play a key role in enhancing reactivity under the studied conditions.

FTIR analysis also revealed differences in the extent of surface oxidation occurring in virgin and post-consumer LDPE under the same conditions. Spectra of the PC-LDPE after oxidative treatment with the homogeneous catalyst showed the typical LDPE bands at 720, 1375, 1461, 1471, 2850 and 2930 cm^{-1}, as previously described, for both types of plastic. Importantly, the post-consumer LDPE reveal new absorption bands

at 3295 and 3070 cm^{-1} which are assigned to the N-H stretching peak and hydrogen bonded hydroxyl group, respectively. A peak at 1635 cm^{-1} characteristic of the carbonyl group (C=O), also appears. The peaks at 1540 and 1373 cm^{-1}, corresponding to the asymmetric and symmetric carboxylate stretching vibrations (COO^-), indicate the presence of carboxylic acid-derived functional groups. The broad C-O stretching modes across 1260-900 cm^{-1}, further support the presence of oxygen containing functional groups (alcohol/ acid/ ester-type moieties) on the polymer surface. Collectively, these changes (Figure 14) indicate surface oxidation of PC-LDPE under the applied conditions.

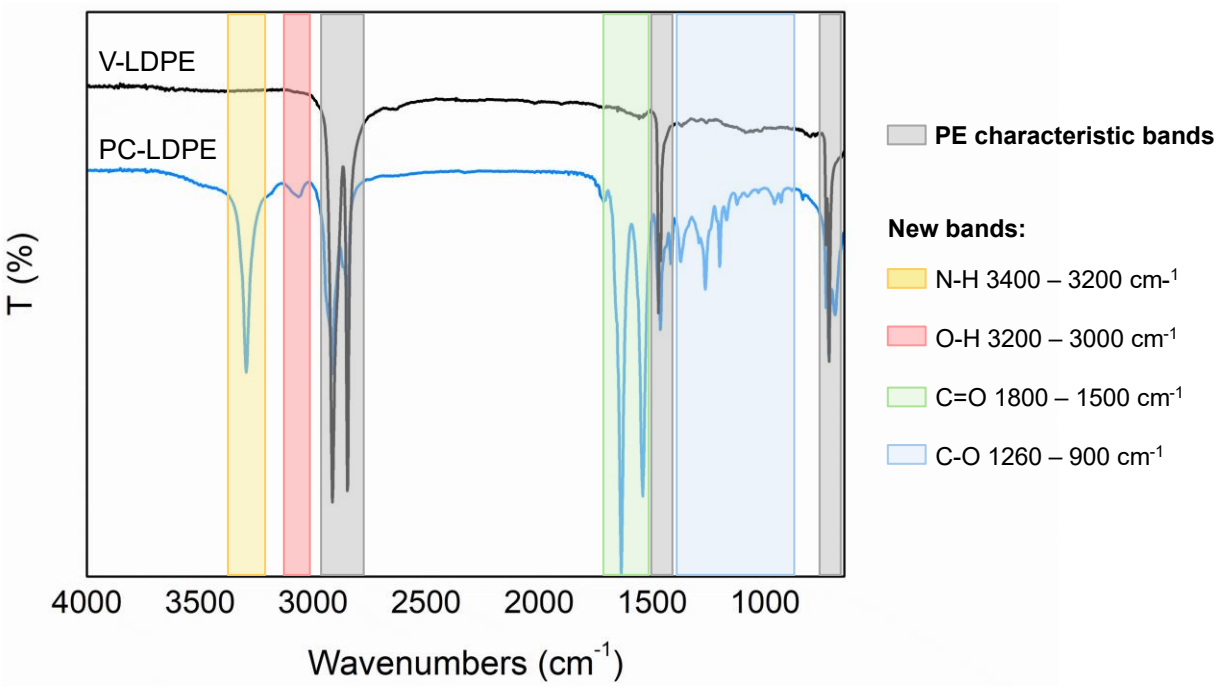


Figure 14. FTIR spectra of virgin and post-consumer LDPE after reaction with the same homogeneous catalyst (Co and Mn acetate). The virgin LDPE shows no evidence of chemical functionalisation, while post-consumer LDPE displays a sharp N-H stretching peak (3500-3300 cm^{-1}), O-H band (3100-3000 cm^{-1}), carbonyl peaks (1800-1500 cm^{-1}), and C-O stretching bands (1260-900 cm^{-1}), consistent with the formation of carboxylic acid functional groups.

To quantify the extent of oxidation, the carbonyl index (CI) was calculated using the specific area under band (SAUB) method from Almond *et al.*[65], taking the 1635 cm^{-1} (carbonyl region feature) normalised to 1471 cm^{-1} (CH_2 bend). While the pristine LDPE had a CI of 0, PC-LDPE had CI of 4.8, indicating a substantially higher degree of surface oxidation for the post-consumer polymer.

Mechanistically, the enhanced surface oxidation and higher mass loss observed for PC-LDPE likely reflect the influence of additives in packaging plastics resulting in additive-assisted oxidation. Additives such as pro-oxidant residues, metal stearates, fillers like talc or calcium carbonate, or pre-existing defects in PC-LDPE may lower H-abstraction barriers, thereby accelerating radical autoxidation and chain scission. The formation of O-containing groups also increase hydrophilicity at the surface and susceptibility to further degradation, aligning with the observed reactivity.

Preliminary side-by-side experiments were conducted on both V-LDPE resin and PC-LDPE to evaluate their thermo-oxidative degradation behaviour. The experiments established that the post-consumer samples yielded particularly interesting results, likely influenced by the presence of additives, stabilisers, or prior processing history. Given that most real-world plastic waste originates from post-consumer sources and recognising that many academic studies focus on pure polymeric materials, the remainder of the investigation focused on PC-LDPE to maximise the practical relevance of the findings.

3.2.4 Time Optimisation of the Degradation Reaction

To evaluate the influence of time on the extent of LDPE degradation, a series of time-screening experiments were conducted using the $MnFe_2O_4$ catalyst. Initially, a 5 h reaction time under catalytic conditions was performed based on the work done by Sullivan *et al.* After 5h, 33 % mass loss was achieved and clear evidence of surface functionalisation was seen with CI = 0.7. Extending the reaction time to 8 h did not increase mass loss further (32 %), however, the CI increased to 1, consistent with broadening of the carbonyl region in the FTIR and signifying a higher degree of surface oxidation. Reducing the reaction time to 3 h reaction also produced a similar mass loss of 32 % with a lower CI = 0.4. A further detailed time series (2 h, 1 h, 30 min and 15 min) indicated that mass loss remained approximately constant (~29–33 %) across this window, whereas CI varied and did not show a consistent trend, but were typically higher at the shorter reaction times as shown in Table 4**.** The data indicates an early plateau in bulk conversion, suggesting that removal of oxidised fragments becomes time-independent under the chosen conditions. In contrast, surface oxidation evolves differently with carbonyl functionalities accumulating rapidly at shorter times (Figure 15) before the surface signal diminishes at longer reaction times. While the mechanism for the observation is unclear, this decoupling of CI from mass loss may be due to (i) detachment or solubilisation of oxidised surface layers, which lowers the residual surface carbonyl signal, or (ii) morphological changes that, as previously highlighted, restrict reagent access and slow further surface functionalisation.

It is also worth noting that while the CI is a widely used and convenient, semi-quantitative assessment of surface oxidation, it is ultimately an indicative metric

sensitive to baseline and thickness effects. Additionally, post-consumer plastics will exhibit regional heterogeneity in formulation, additives and prior weathering, so observed CI variability may reflect feedstock differences rather than reaction conditions.

Table 4. The effect of reaction time on mass loss and carbonyl index (CI) of PC-LDPE. The mass loss reaches a fundamental plateau at ca. 30 % and the carbonyl index does not exhibit a consistent trend over time, fluctuating without clear correlation to reaction duration. A representative standard deviation was determined as 30.9 ± 2 % (n=3) from a key reaction to indicate the general variability in mass loss.

Conditions: PC-LDPE, 120 °C, varying reaction time, $MnFe_2O_4$ (9.6 wt%), NHPI (11.2 wt%), CI area = 1850-1650 cm^{-1} / 1470 cm^{-1}.

Reaction Time	Mass loss (%)	Carbonyl Index (CI)
8 h	31.5	1.5
5 h	32.9	0.7
3 h	31.9	0.4
2 h	32.7	4.3
1 h	30.9	1.9
30 min	28.9	6.0
15 min	29.6	6.2

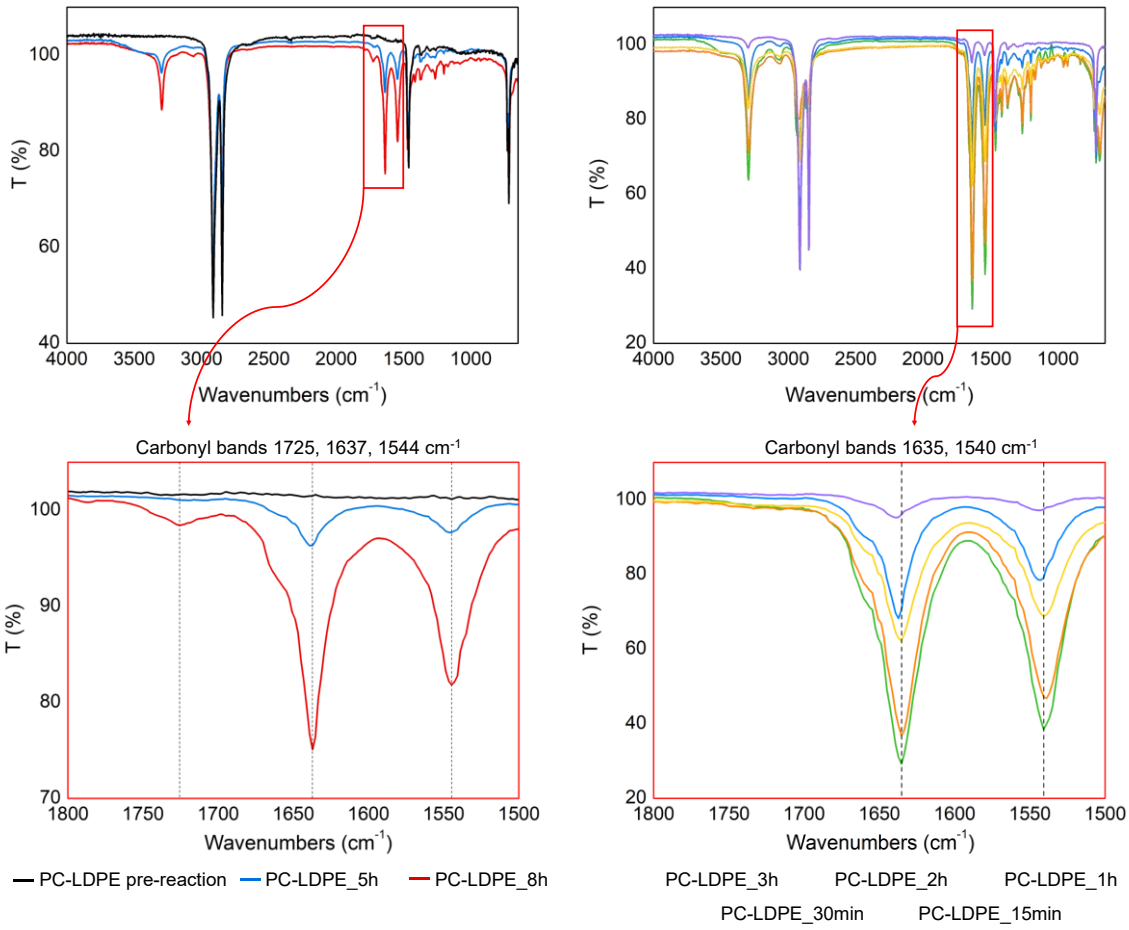


Figure 15. Comparative FTIR spectra of post-consumer LDPE reacted with $MnFe_2O_4$ heterogeneous catalyst at 120 °C over varying time intervals. Left: unreacted PC-LDPE (black), 5 h (blue), 8 h (red); right: 15 min (green), 30 min (orange), 1 h (blue), 2 h (yellow), and 3 h (purple).

Conditions: PC-LDPE, 120 °C, varying reaction time, $MnFe_2O_4$ (9.6 wt%), NHPI (11.2 wt%), CI area = 1850-1650 cm^{-1} / 1470 cm^{-1}.

To investigate whether the catalytic system was necessary at such short durations, additional experiments were conducted at 1h, 30 min and 15 min without the metal catalyst or NHPI. Remarkably, these reactions still exhibited ~30 % mass loss, indicating that thermal treatment alone in acetic acid at 120 °C was sufficient to induce a significant degree of degradation within a short timeframe. These results suggest that the reaction may reach a fundamental plateau quickly, after which

additional time or catalyst offers no significant advantage. One possible explanation is that rapid oxidation occurs in the more accessible amorphous regions of PC-LDPE, which contain greater free volume and facilitate the incorporation of oxygen, whereas the highly crystalline areas of the sample may resist degradation due to the possibility of cross-linking between the carbon chains, effectively reducing chain cleavage along the polymer backbone[66,67]. Additionally, compared to V-LDPE, PC-LDPE possesses a lower degree of crystallinity due to the heterogeneity of the polymer matrix influenced by additives, previous processing history, etc. This structural difference likely accounts for the lower mass loss and greater resistance to thermo-oxidative degradation observed for V-LDPE. Another hypothesis involves the role of additives present in post-consumer LDPE. Since additives such as plasticisers are not chemically bound to the polymer, it is possible they may migrate or leach out of the polymer matrix, thereby reducing crystallinity, and initially react with the acetic acid or facilitate the formation of reactive species[68]. Once these reactive additives are depleted, the system may no longer support further degradation, effectively limiting the extent of polymer breakdown. This implies that the degradation rate—and limit—could be governed more by additive content rather than the composition of the polymer, highlighting the complexity and variability in post-consumer plastics.

3.2.5 Catalyst and NHPI Loading

The influence of catalyst concentration was examined using Mn–Fe spinel at 0 wt%, 5 wt%, 9.6 wt%, and 15 wt% loadings, with all other conditions held at the standard conditions—120 °C, 5 h, sealed pressure tubes, acetic acid solvent, NHPI (11.2 wt%).

Mass loss obtained at all loadings was ~30 % which was surprising as previous work in microwave depolymerisation showed the oxidation reaction to be sensitive to catalyst loading. A control reaction (0 wt%), suggests that bulk conversion is insensitive to catalyst concentration within this range.

To exclude artefacts from trace metal contamination, all glassware and stir bars were cleaned with aqua regia prior to repeating the experiments. The mass loss again remained ~30 %, confirming that the degradation observed in blanks was not attributable to residual metals. This indicated that the catalysts suppress surface functionalisation, potentially by altering radical lifetimes or promoting non-productive peroxide decomposition, as supported by FTIR analysis (Figure 16) revealing an inverse trend between catalyst loading and surface oxidation. The 0 wt% sample (NHPI present) exhibited the strongest carbonyl features (CI ≈ 3.8), whereas increasing the catalyst loading produced a progressive decrease in the intensity of these bands. At the same time, the CH_2 stretching bands at 2915 and 2846 cm^{-1} diminished with increasing oxidation, consistent with consumption of aliphatic C–H, chain scission and oxygen incorporation.

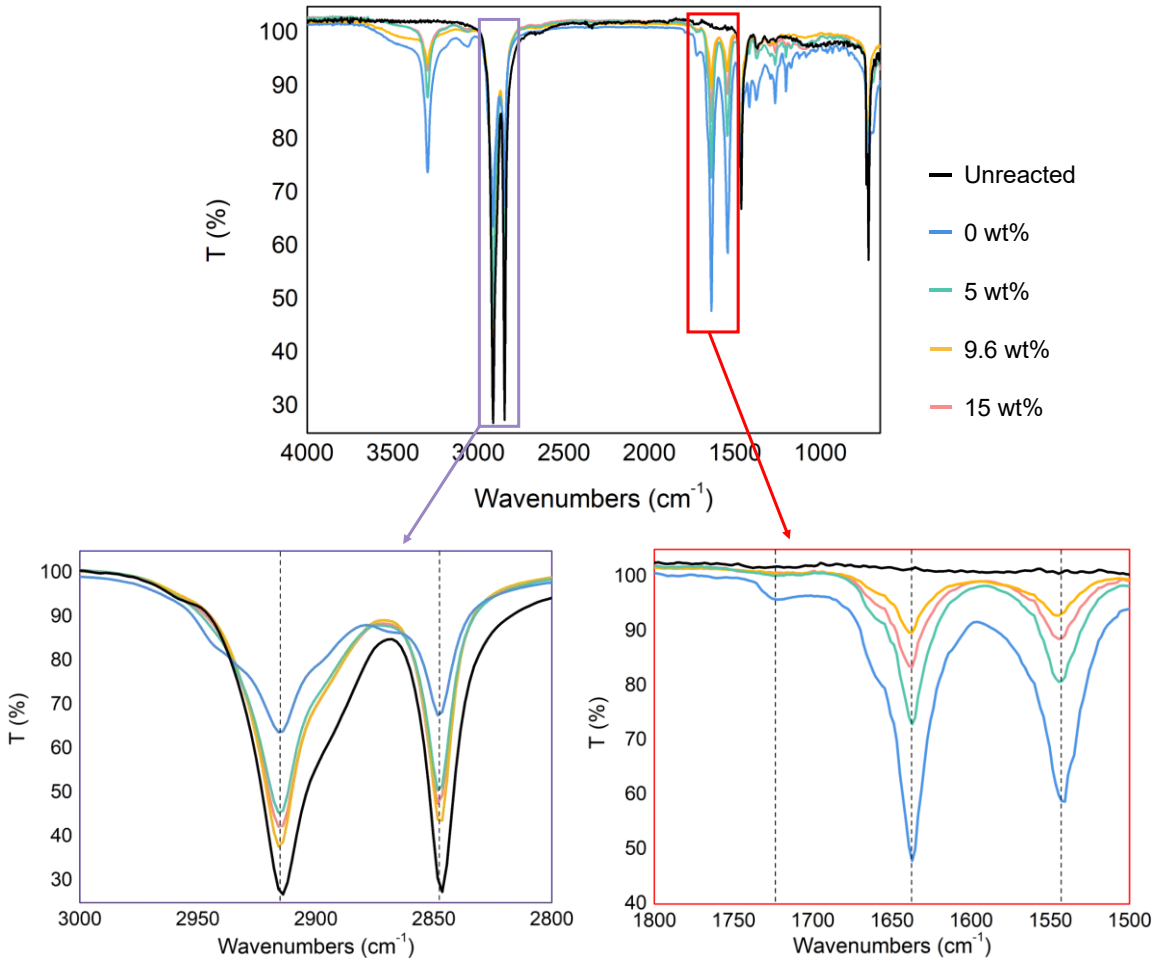


Figure 16. FTIR spectra of LDPE before (black) and after reaction with different catalyst loadings: 0 wt% (blue), 5 wt% (green), 9.6 wt% (yellow), and 15 wt% (red) shows increasing oxidation with decreasing catalyst loading and that the highest degree of functionalisation stems from reaction with no catalyst. A corresponding decrease in CH_2 stretching peaks suggests progressive breakdown of the polymer backbone during oxidation.

Conditions: PC-LDPE, 120 °C, 5 h, $MnFe_2O_4$ (varying loading), NHPI (11.2 wt%), CI area = 1850-1650 cm^{-1} / 1470 cm^{-1}.

To elucidate the role of NHPI in LDPE degradation, reactions were performed at 0 wt%, 11.2 wt%, and 20 wt% NHPI (relative to polymer), keeping all other variables constant (Mn–Fe catalyst 9.6 wt%, acetic acid, 120 °C, 5 h, sealed pressure tubes). Across all reactions—including the 0 wt% NHPI control, the mass loss was ≈30 %. FTIR analysis (Figure 17) revealed pronounced differences in surface oxidation despite the

similar bulk conversion. In the absence of NHPI, the spectra exhibited the strongest carbonyl-region features (e.g., bands at ~1637 and ~1542 cm^{-1}) indicating extensive oxidative functionalisation. At 11.2 wt% NHPI, surface oxidation was minimal, while at 20 wt% NHPI an intermediate degree of oxidation was observed as indicated by FTIR. The lack of a strict correlation between CH_2 stretching, carbonyl growth and NHPI loading may indicate an oxidation pathway beyond simple backbone consumption but is also likely due to polymer variation in post-consumer LDPE. As discussed earlier, interpretation of the CI should be done with caution, as variability in the metric—especially for post-consumer plastics, may reflect feedstock heterogeneity as much as reaction conditions.

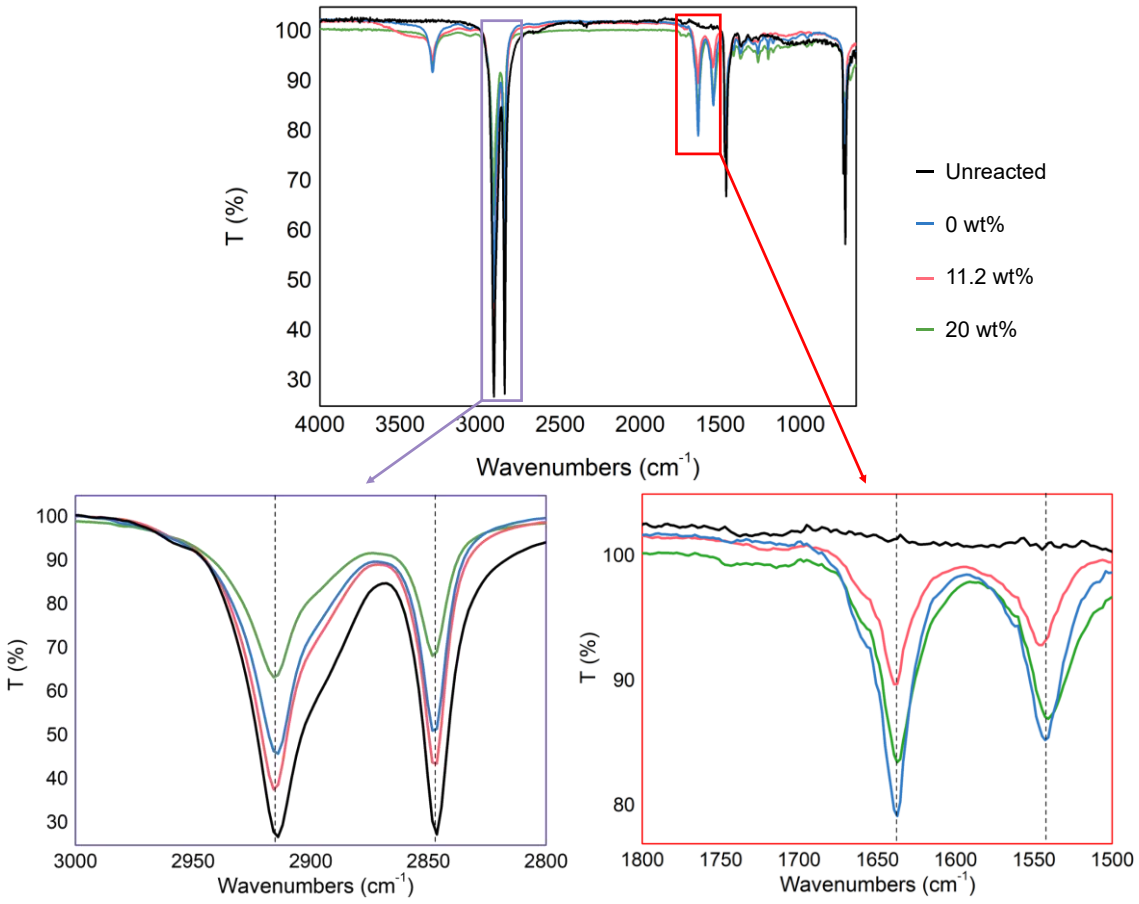


Figure 17. FTIR spectra of LDPE following reaction at 120 °C for 5 h (fixed Mn-Fe catalyst loading) reacting with varying NHPI loading: 0 wt%, 11.2 wt% and 20 wt%. Despite similar bulk mass loss (~30 %) across all samples, the highest oxidation was

observed in the control (no NHPI), minimal levels at 11.2 wt% and intermediate levels at 20 wt% NHPI.

Conditions: PC-LDPE, 120 °C, 5 h, $MnFe_2O_4$ (9.6 wt%), varying NHPI loading, CI area = 1850-1650 cm^{-1} / 1470 cm^{-1}.

Regardless of the CI variability, the experiments clearly confirm that under the present conditions, acetic acid alone can functionalise the LDPE surface to a substantial extent and induce significant mass loss (30 %), however mass losses over 33 % were not observed, even after prolonged reaction times. A plausible explanation for the similar mass loss is that degradation is predominantly thermally driven in this regime, with the catalytic PINO pathway contributing less to overall bulk conversion than anticipated. Moreover, because the reactions were conducted in sealed tubes, the process relies on headspace air (≈21 % O_2, 0.26 mmol O_2); once the available O_2 is consumed, further generation of PINO (and subsequent oxidation) may be limited, imposing an apparent ceiling in mass loss (~30 %) independent of NHPI loading (see Experimental section for headspace oxygen calculation).

3.2.6 Probing Oxidant Availability with Hydrogen Peroxide (H_2O_2)

It was hypothesised that the fundamental limit of 30 % in mass loss could be due to the reactions being carried out under atmospheric conditions in a sealed vessel, where the reaction relies solely on the air (0.26 mmol O_2) trapped inside the vessel and once the oxygen is consumed, there is no replenishment, effectively hindering the formation of the PINO species. To test whether oxidant availability limits conversion, H_2O_2 (2 wt% solution, 1 mL) was introduced in a 1 h reaction under

otherwise standard conditions with PC-LDPE, either as a single initial dose or by incremental dosing during the run (catalyst and NHPI present in both cases). No increase in mass loss was observed relative to the peroxide-free control.

FTIR analysis shown in Figure 18 also provided additional insight. The control (no H_2O_2) exhibited strong carbonyl absorption with CI ≈ 1.9. When H_2O_2 was added all at once, CI decreased to ≈1.1, consistent with rapid peroxide decomposition and a corresponding reduction in net oxidative functionalisation. Incremental H_2O_2 addition produced heterogeneous surface oxidation within the same specimen having widely different values indicating non-uniform local radical environments. Notably, a new band at ~1750 cm^{-1}, was observed suggesting formation of additional oxidised species, likely from a Fenton-type mechanism, indicating that multiple pathways may operate concurrently. As with the NHPI series, there was no strict one-to-one correspondence between attenuation of CH_2 stretching and growth of carbonyl bands.

Collectively, these results indicate that adding H_2O_2 is not an effective substitute for ambient molecular oxygen under the present conditions, possibly due to unfavourable radical generation kinetics. As bulk conversion does not increase with peroxide dosing, oxygen availability is unlikely to be the primary limiter of mass loss in this reaction and other factors such as mass-transfer constraints or interactions between polymer additives and reagents are more likely to be the reason for the observed ceiling in mass loss. These results further support that LDPE conversion proceeds mainly via thermally driven, solvent-assisted pathways rather than a radical based reactive oxygen species from the PINO species.

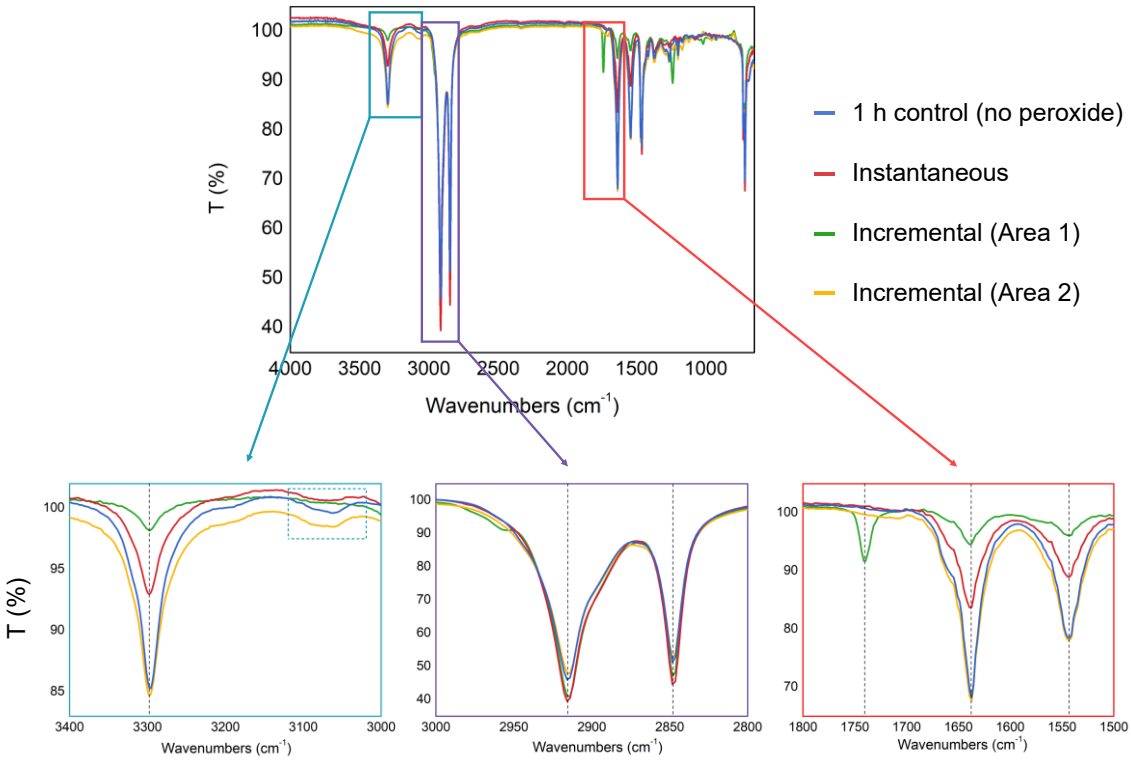


Figure 18. FTIR spectra of PC-LDPE after 1 h reactions under different conditions: control without peroxide (blue line), peroxide added as single initial dose (red line), peroxide added incrementally with analysis of two different areas of the same sample (green and yellow line).

Conditions: PC-LDPE, 120 °C, 1 h, $MnFe_2O_4$ (9.6 wt%), NHPI (11.2 wt%), H_2O_2 (2 wt%) CI area = 1850-1650 cm^{-1} / 1470 cm^{-1}.

3.3 Effect of a Second Thermal Treatment

To investigate whether partially degraded LDPE remains reactive under standard conditions, (120 °C, Mn-Fe catalyst (9.6 wt%), NHPI (11.2 wt%)) the previously reacted polymer residues were isolated by filtration, dried and subjected to a second reaction under identical conditions. No additional mass loss was observed upon re-treatment, indicating that no further degradation had occurred. FTIR analysis (Figure 19) reveals markedly different surface chemistries after the two oxidising treatments. For PC-LDPE initially treated for 5 h (Figure 19 (a)), pronounced oxidation peaks were

observed at ~3300 cm^{-1} (N-H stretching), 1620 cm^{-1} and 1540 cm^{-1} (carbonyl-related absorptions). After the second treatment, these features were absent, replaced instead by a distinct peak at 1739 cm^{-1}, indicative of a different carbonyl environment. The same observation can be seen in Figure 19 (b) for the 1 h reaction in the presence of catalyst and NHPI, suggesting that labile oxygenated groups formed in the initial cycle decompose, desorb, or rearrange to more thermodynamically stable carbonyl species during re-treatment. Finally, when the initial reaction was performed for 1 h without catalyst or NHPI, the spectra of both samples were broadly similar (Figure 19 (c)), but with lower peak intensities after the second treatment.

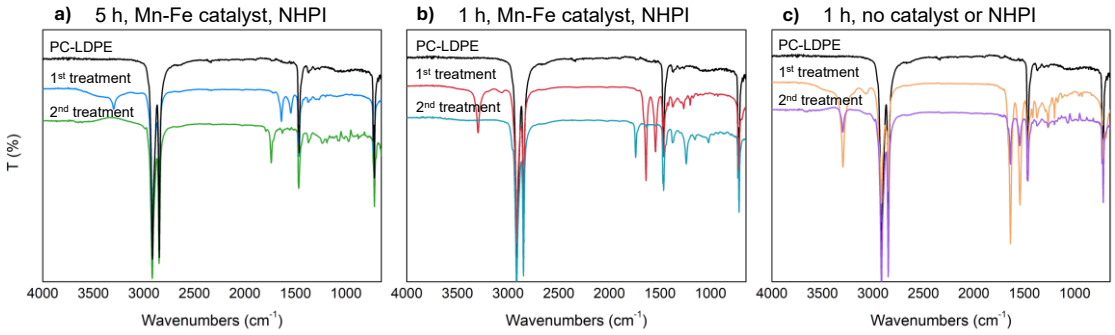


Figure 19. Effect of a second thermo-oxidative treatment on PC-LDPE under different conditions: **(a)** 5 h, catalyst, NHPI; **(b)** 1 h, catalyst, NHPI; **(c)** 1 h, no catalyst or NHPI. In the presence of catalyst and NHPI, the emergence of a new peak 1739 cm^{-1} was observed indicating a shift to more thermodynamically stable carbonyl species. While in the absence of catalyst and NHPI, only lower intensity peaks were seen after the second cycle.

Conditions: PC-LDPE, 120 °C, varying time, Co/Mn homogeneous catalyst (4.85 wt%/4.75 wt%, respectively) and $CoFe_2O_4$ heterogeneous catalyst (9.6 wt%), NHPI (11.2 wt%).

These results indicate that the fraction of LDPE susceptible to rapid thermo-oxidative transformation is largely consumed during the first cycle. The residue appears

resistant to further reaction, likely due to one of more contributing factors such as more crystalline domains, or densified, congealed regions leading to lower surface area with limited reagent access. While no mass loss is observed, changes in surface chemistry can be seen after treatment only in the presence of the catalyst and NHPI. Finally, the role of additives is likely to play a role in the observed reactivity: additive depletion in the first cycle may curtail further chemistry in the second, particularly if early-stage reactivity is additive-assisted and this would be consistent with the negligible mass observed after re-treatment.

3.4 High Performance Liquid Chromatography (HPLC) Analysis

High performance liquid chromatography was used to identify low molecular weight carboxylic acids formed during the thermo-oxidative degradation of LDPE. Calibration curves were established for selected carboxylic acid standards where the concentration was given, and the amount of each product was calculated against these calibration curves (Figure 20). Retention times for these acids, obtained from standards of carboxylic acids, are summarised in Table 5 which are used to identify the products from the reaction mixtures.

- **Analytical Limitations:** Although quantitative analysis was attempted, the use of acetic acid as the reaction medium resulted in a very large acetic acid peak, which obscured or even masked nearby peaks. Therefore, HPLC was employed mainly as a qualitative analysis technique. Higher dilutions were explored, however, the concentrations of the products decreased significantly, reducing their detectability.
- **Practical solutions:** HPLC alone is insufficient for fully characterising the liquid products. Complementary approaches such as, solid phase extraction (SPE), different size-exclusion column/adjusting pH, derivatisation followed by gas chromatography-mass spectrometry (GC-MS) may provide a more comprehensive picture of product distribution.

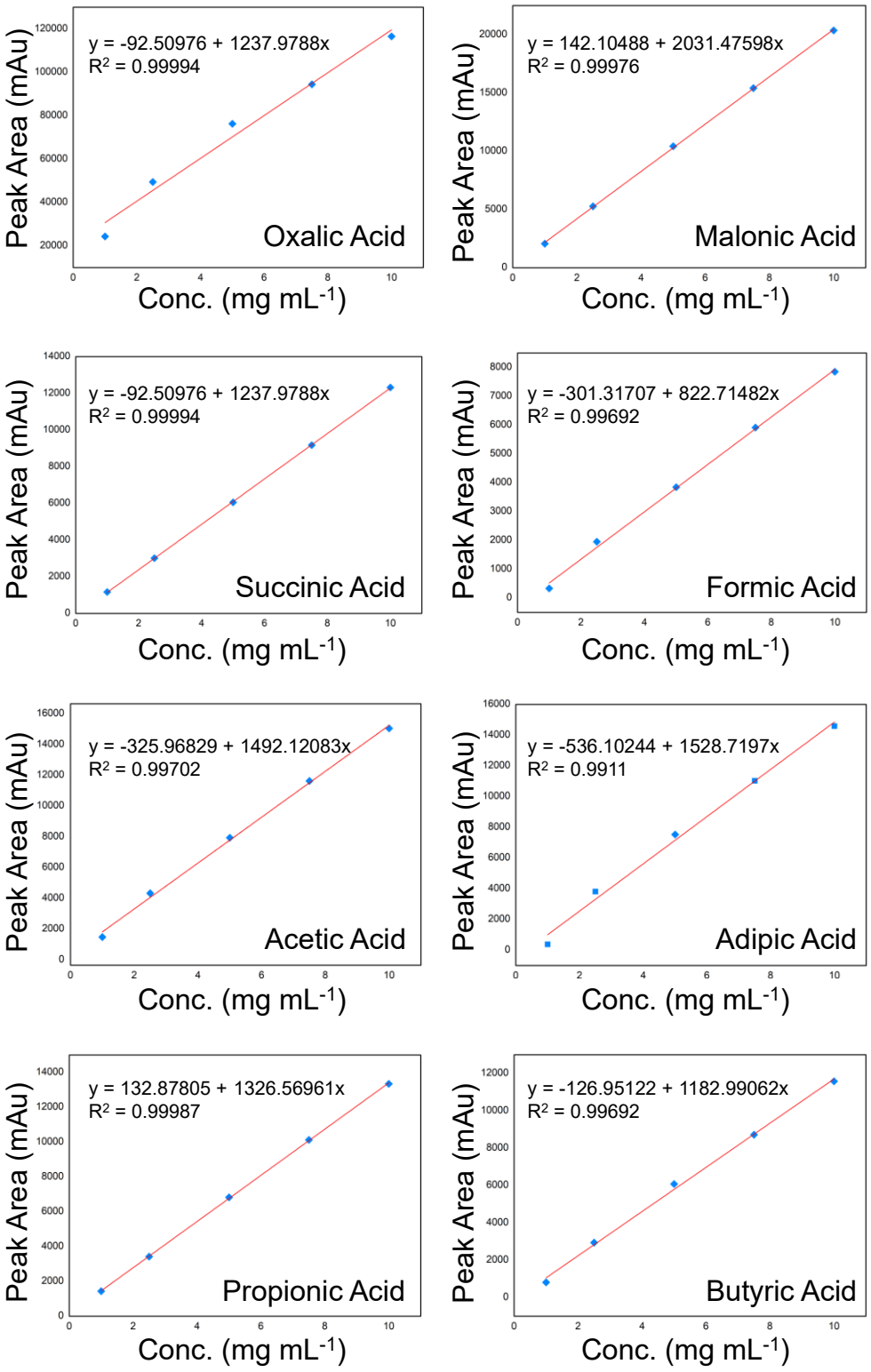
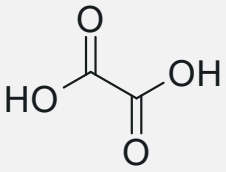
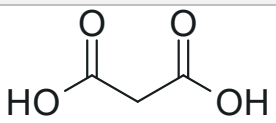
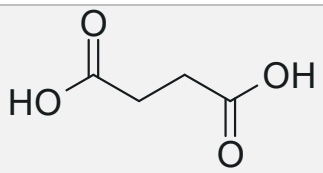
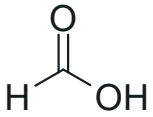
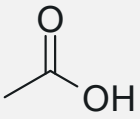
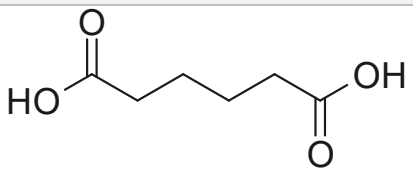
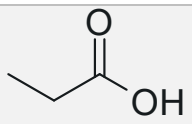
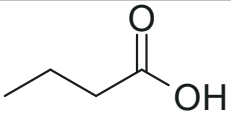
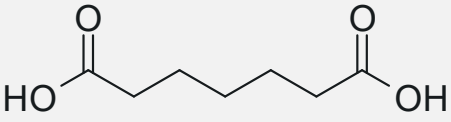


Figure 20. Calibration curves for the different carboxylic acids obtained from HPLC. All curves exhibited good linearity across the calibration range.

Table 5. Retention times in minutes for each end-product

Retention Time (min)	Product	Structure
11.0	Oxalic acid	
13.0	Malonic acid	
15.4	Succinic acid	
17.2	Formic acid	
18.9	Acetic acid	
21.0	Adipic acid	
23.5	Propionic acid	
28.8	Butyric acid	
32.3	Pimelic acid	

Virgin LDPE—homogeneous Co/Mn system:

HPLC analysis of the liquid products from the reaction with homogeneous Co/Mn acetate catalyst revealed two early peaks at 7.2 and 8.4 min which are attributed to metal contamination from the catalyst and the solvent peak, respectively. Peaks corresponding to succinic acid and formic acid were detected, along with the large acetic acid peak with an area of 209,300 milli-Absorbance units (mAu). The acetic-acid peak exhibited splitting, consistent with overload at a modest 2× dilution. Additional minor components were visible, but reliable quantification was achieved only for succinic acid (≈3 mg/ 10 mL) and formic acid (≈8 mg /10 mL), consistent with the low mass observed for the pristine LDPE.

Virgin LDPE—heterogeneous Co–Fe system:

For the heterogeneous Co-Fe system, major assigned products included succinic, formic, and butyric acid. Additional minor peaks were identified at ~11 min, 22.7 min and 31.7 min, which correspond to malonic, adipic and pimelic acid, respectively. Peak interferences such as impurities or a broad acetic acid peak, which typically elutes over a 2–3 minute window can interact with the UV detector and alter retention behaviour, leading to slight shifts in apparent elution times. As in the homogeneous case, the acetic-acid peak dominated the chromatogram, limiting both identification and quantitation of minor species, particularly glutaric acid, which elutes close to acetic acid under the present method (RT ≈ 18.2 min). The chromatograms of the reaction mixtures from the degradation of virgin LDPE with

homogeneous and heterogeneous catalysts can be seen in Figure 21 (A) and (B), respectively.

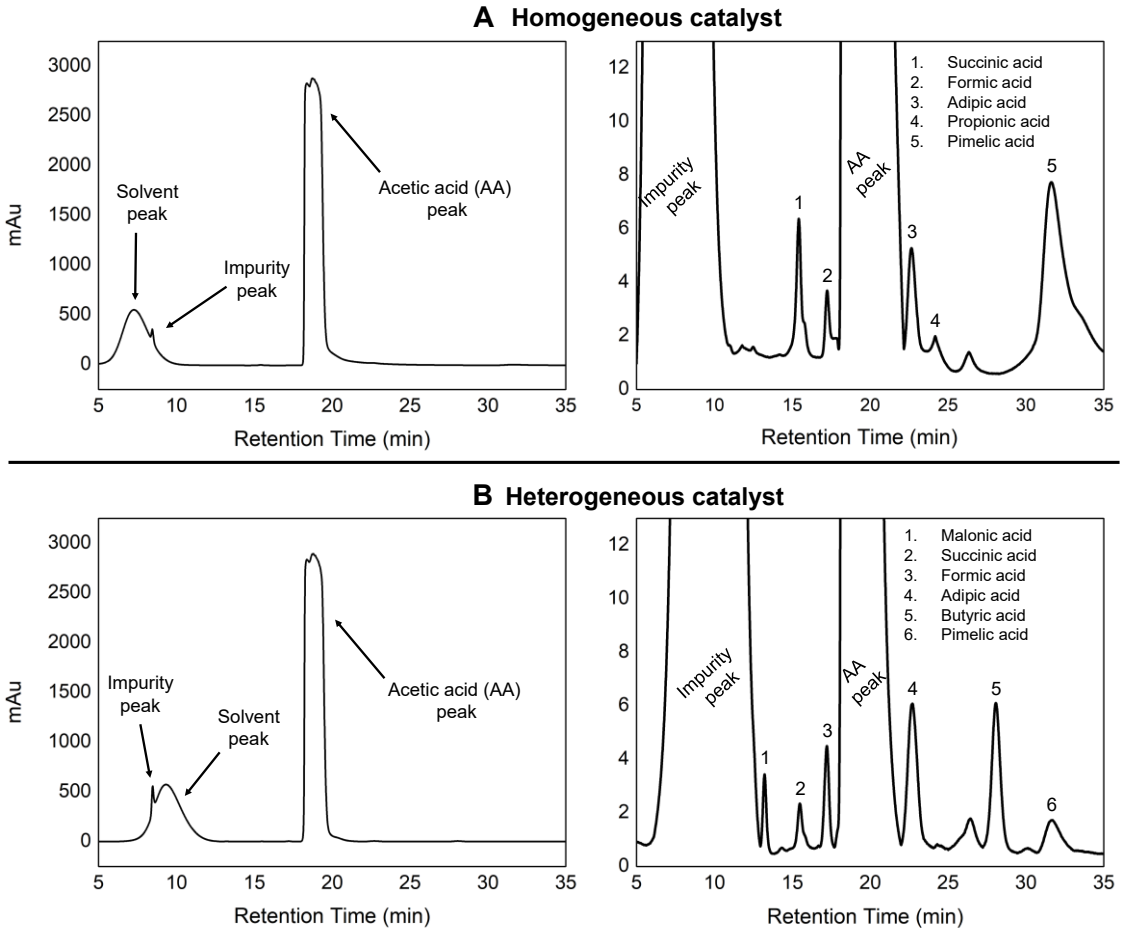


Figure 21. Qualitative HPLC chromatograms comparing the products of V-LDPE after reaction with two different catalysts. **(A)** homogeneous Co/Mn acetate catalyst and **(B)** heterogeneous Co-Fe catalyst.

Conditions: V-LDPE, 120 °C, 5 h, Co/Mn homogeneous catalyst (4.85 wt%/4.75 wt%, respectively) and $CoFe_2O_4$ heterogeneous catalyst (9.6 wt%), NHPI (11.2 wt%).

Post-consumer LDPE (PC-LDPE)—homogeneous Co/Mn system:

Using the same catalyst on post-consumer plastic, the product distribution resembled that from virgin LDPE, with formic and succinic acids as the principal assigned peaks. Despite intense surface oxidation in FTIR and reasonably good mass loss (30 %), only

small amounts of soluble acids were detected by HPLC. Irregularities on the baseline were also observed with the PC-LDPE as seen in Figure 22. This can be attributed to the partial blockage or fouling of the column due to particulates or additives from the PC-LDPE. The overwhelming acetic-acid signal and co-elution constraints restrict quantitative interpretation but nonetheless, HPLC provides qualitative evidence for the formation of formic, adipic, and succinic acids across conditions.

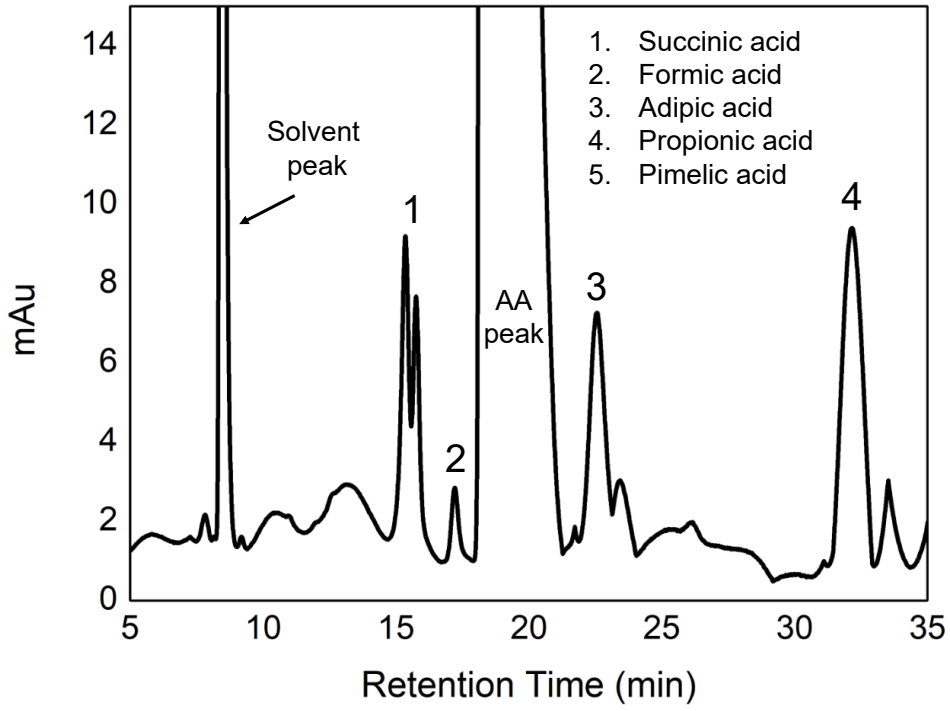


Figure 22. Qualitative HPLC chromatogram of PC-LDPE after reaction with homogeneous Co/Mn acetate catalyst.

Conditions: PC-LDPE, 120 °C, 5 h, Co/Mn acetate catalyst (4.85 wt%/4.75 wt%, respectively), NHPI (11.2 wt%).

3.4.1 Effect of Mn–Fe heterogeneous catalyst and NHPI loading on product distribution for PC-LDPE

When investigating the effect of the Mn-Fe catalyst loading on product distribution, HPLC results (Figure 23) show a clear trend where increasing catalyst loading leads to a wider product profile. At 0 wt% catalyst, only formic acid was identifiable with an unresolved peak at 21-22 min. In the absence of catalytic sites, minimal product diversity is observed. At 5 wt%, additional peaks corresponding to oxalic, succinic, adipic and propionic acid were identified. At 9.6 and 15 wt% further product peaks are identified including malonic, pimelic and butyric acid. This is particularly noteworthy, because the mass loss was relatively constant in all catalyst loadings tested, yet greater product diversity was favoured at higher catalyst loadings. It was not possible to do accurate quantification of the acid yield, however, these results suggest that increasing the Mn–Fe catalyst loading, increases the probability of radical generation and subsequent scission events along the backbone, giving rise to a wider range of low molecular-weight acids. In parallel, FTIR of the solid residues showed a progressive decrease in surface oxygen functionalities with rising catalyst loading, implying that higher loadings favour rapid detachment of oxidised fragments into solution rather than their accumulation on the polymer surface.

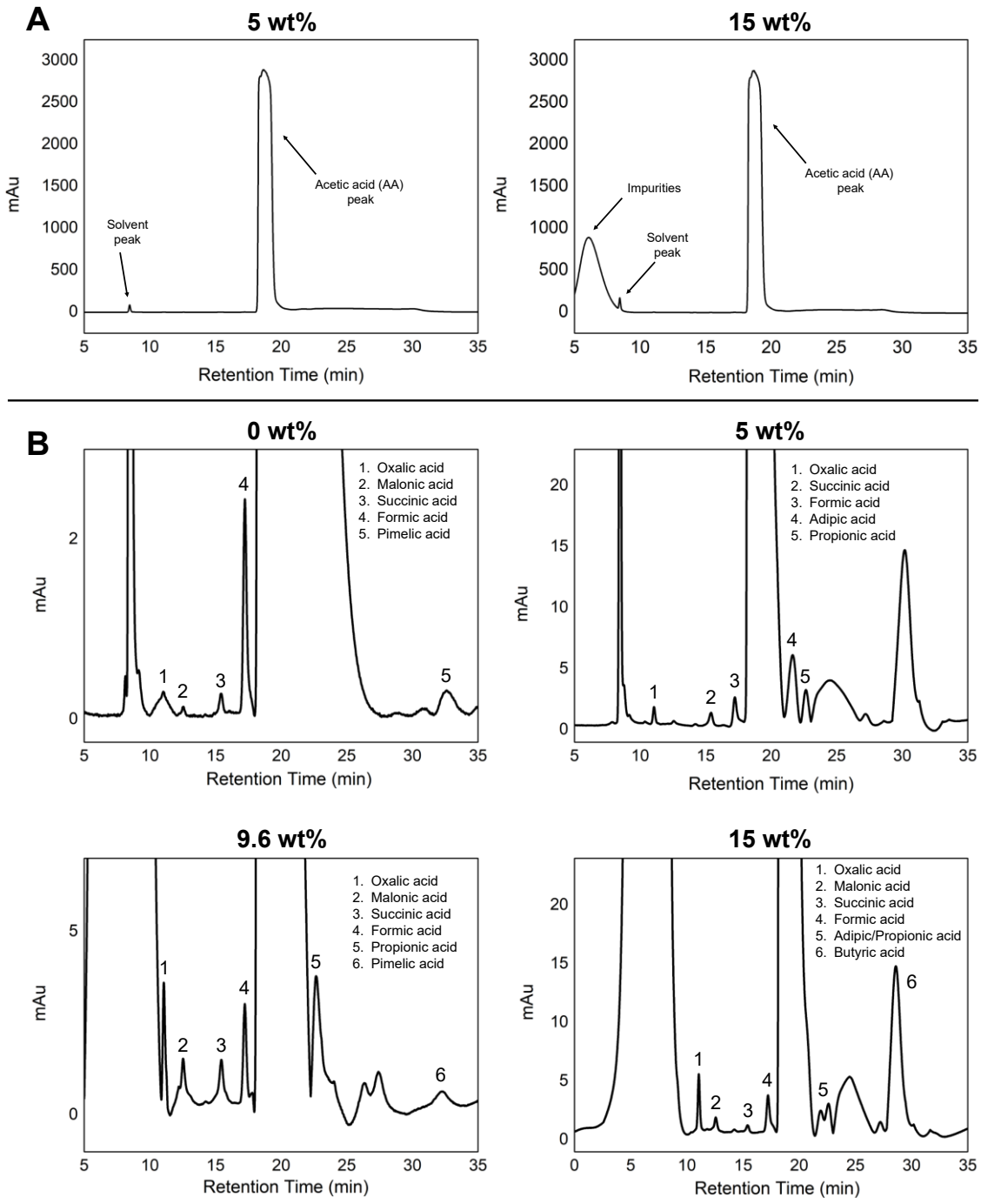


Figure 23. Qualitative comparison of HPLC chromatograms for PC-LDPE showing **(A)** the absence and presence of an impurity peak at lower (5 wt%) and higher (15 wt%) catalyst loadings, respectively, and **(B)** the effect of different catalyst loadings on the product distribution after reaction. Increasing catalyst loading seem to increase the product profile with the most compounds being identified at 9.6 and 15 wt% Mn-Fe catalyst.

Conditions: PC-LDPE, 120 °C, 5 h, varying $MnFe_2O_4$ catalyst loading, NHPI (11.2 wt%).

1 h reactions of PC-LDPE in the absence of catalyst and NHPI produced a narrow product distribution, typically formic acid (17.2 min) and a broad unresolved feature at 21–22 min (Figure 24 (a)). In the absence of catalytically active sites, the higher activation barrier slows thermo-oxidative cleavage, yielding fewer soluble products. Direct comparison with a 1 h reaction with catalyst and NHPI showed a broader profile including succinic and oxalic acids but with the same unresolved peaks (Figure 24 (b)). Without these active sites, reactive intermediates may undergo side reactions forming insoluble residues rather than forming soluble low-molecular weight acid products[69]. These intermediates may also remain bound to the polymer matrix as observed in FTIR analysis where the surface of PC-LDPE is highly functionalised with oxygen groups. This leads to the hypothesis that under these conditions (120 °C, catalyst, and NHPI), the acetic acid solvent itself may undergo decomposition, forming low molecular weight carboxylic acids which contribute to the observed chromatogram.

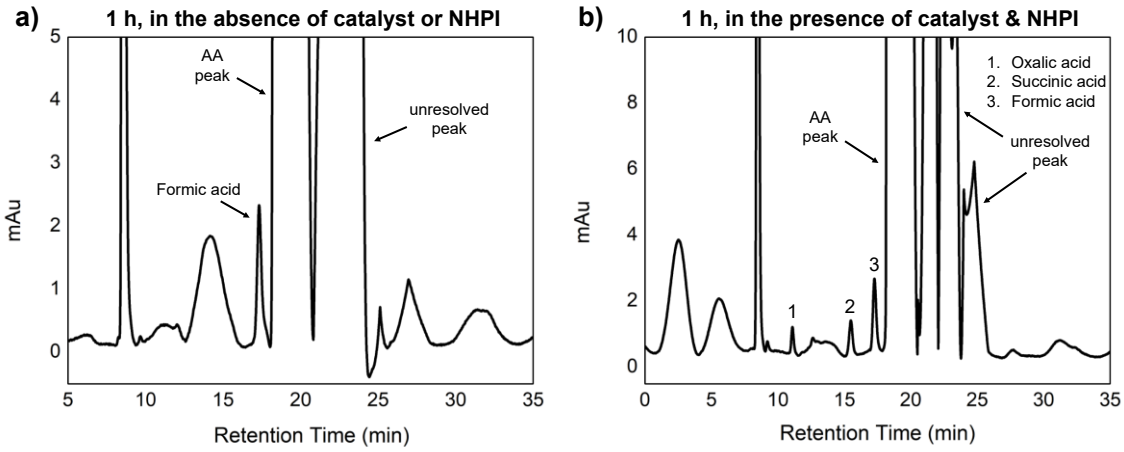


Figure 24. Qualitative HPLC chromatogram of PC-LDPE after a reaction **(a)** with no catalyst or NHPI and **(b)** with catalyst and NHPI. Both showing a narrow product distribution with formic acid at 17.2 min and an unresolved peak at 21-22 min.

Conditions: PC-LDPE, 120 °C, 1 h, $MnFe_2O_4$ (9.6 wt%), NHPI (11.2 wt%).

Varying NHPI (0, 11.2, 20 wt% relative to polymer) had little effect on the product spectrum: all chromatograms displayed peaks at ~11.0 min and ~17.2 min (assigned to oxalic and formic acid, respectively). Additional unquantifiable peaks appeared upon magnification at ~15.2, ~26.1, and ~30.9 min, but their presence was not systematically correlated with NHPI loading. These observations indicate that NHPI does not substantially alter the degradation pathway under the present conditions.

3.4.2 Second Acetolysis Treatment

To investigate whether additional soluble products would be formed from partially oxidised material, previously reacted PC-LDPE was subjected to a second acetolysis under identical conditions. Three samples were evaluated: a 5 h reaction in the presence of the Mn-Fe catalyst and NHPI, a 1 h reaction with the same reagents and a final 1 h reaction without any catalyst or radical initiator. In all cases, no change in mass loss was recorded, however, the second treatment resulted in a broader product distribution (Table 6). This behaviour is consistent with (i) further breakdown of partially oxidised intermediates remaining on the polymer after the first cycle, (ii) reaction at pre-existing oxidation sites/radicals, and (iii) greater exposure of fresh polymer as the matrix opens, increasing the number of accessible cleavage sites.

Table 6. Reaction products detected after a first and second run of the acetolysis reaction with PC-LDPE, with more products generated after a second treatment of the polymer.

Reaction Conditions	Products Detected	
	1st Treatment	2nd Treatment
5 h, Mn-Fe catalyst, NHPI	Oxalic, formic acid	Oxalic, malonic, succinic, formic, pimelic acid
1 h, Mn-Fe catalyst, NHPI	Succinic, formic, adipic, propionic acid	Oxalic, malonic, succinic, formic acid
1 h, no catalyst or NHPI	Formic acid	Formic and propionic acid

Collectively, the qualitative HPLC results demonstrate that catalyst type, presence of a radical initiator, and loadings influence not only the extent of LDPE transformation, but also the diversity of soluble products formed during acetolysis at 120 °C. Increasing Mn–Fe loading expands the product profile, whereas NHPI loading has minimal impact on product identity under the present conditions. In catalyst-free reactions, the product spectrum narrows, and intermediates tend to form insoluble residues, consistent with FTIR evidence of high surface functionalisation and limited bond cleavage. A second acetolysis step liberates additional acids, supporting a model in which the first pass generates bound or oligomeric oxygenates that require further treatment for release. Figure 25 below shows a summary schematic of a typical PC-LDPE run, illustrating the initial mass, recovered solid, quantified acids, unassigned dissolved fraction, and uncollected volatiles.

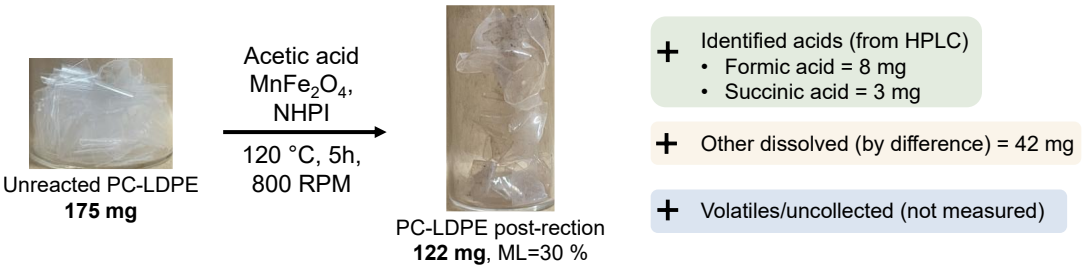


Figure 25. Schematic representation of a typical PC-LDPE run showing the distribution of mass into recovered solid, quantified carboxylic acids, dissolved unassigned products, and collected volatiles.

Methodological limitations of the HPLC prevent detailed analysis of the product distribution profile. Improved quantitation could be pursued in future work via (i) sample clean-up (e.g. solid-phase extraction (SPE) to reduce acetic acid), (ii) alternative separations (ion-exclusion columns or altered mobile-phase pH), and/or (iii) derivatisation/GC-MS to profile a wider range of oxygenates.

3.5 X-Ray Photoelectron Spectroscopy (XPS) Analysis

X-ray photoelectron spectroscopy (XPS) was employed to investigate the surface chemistry of the polymer surface of both virgin LDPE (V-LDPE) and post-consumer LDPE (PC-LDPE) before and after reactions using typical loadings of Mn-Fe catalyst (9.6 wt%) and radical initiator, NHPI (11.2 wt%) at 120 °C. Due to the shallow penetration (approx. 1 nm) of the X-rays, XPS greatly enhances surface sensitivity and determination of different functional groups on the polymer surface. All samples were filtered and washed with deionised water prior to XPS analysis. Survey scans for all samples were collected (Figure 26) to provide a general overview of the elemental

composition and surface modification. The relative atomic concentrations of C, O and N are derived and quantified from the survey scans and is presented in Table 7.

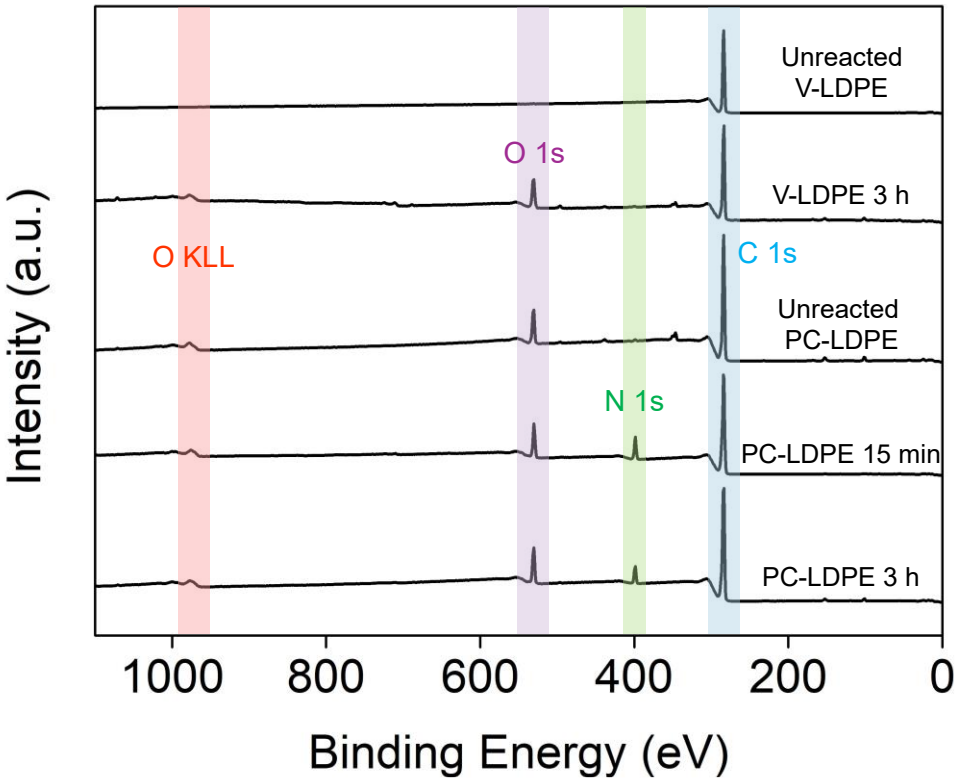


Figure 26. Survey XPS spectra for virgin and post-consumer LDPE samples before reaction (control) and after a 15 min and 3 h reaction. Post-reaction samples have been washed with DI H_2O prior to XPS analysis.

Table 7. Atomic concentrations (%) of the different elements constituting the surface of the virgin and post-consumer LDPE samples from a 15 min and 3 h reaction after washing with DI water.

Samples	Atomic Concentration (%)		
	C 1s	O 1s	N 1s
Unreacted V-LDPE	99.9	0.1	--
V-LDPE 3 h	81.0	12.9	0.7
Unreacted PC-LDPE	84.4	10.6	0.6
PC-LDPE 15 min	79.9	10.3	9.4
PC-LDPE 3 h	81.3	10.3	6.7

The survey spectra and corresponding elemental quantification highlight clear differences in surface composition between V-LDPE and PC-LDPE, both in their pristine state before reaction and after oxidative treatment. The V-LDPE control exhibited no detectable O 1s peak, consistent with a hydrocarbon surface. In contrast, the PC-LDPE before reaction, showed a distinct O 1s peak attributed to oxidative ageing from ambient exposure and/or the presence to polymer additives. Interestingly, an N 1s signal was observed in the post-consumer polymer after reaction, which was not seen for the virgin resin, indicative of a more chemically diverse surface of the PC-LDPE (e.g. additive residues). To gain deeper insight into the chemical states of these elements, high resolution C 1s and O 1s spectra were collected for V-LDPE, while additional N 1s analysis was performed for PC-LDPE.

V-LDPE: chemical-state evolution upon acetolysis

The C 1s and O 1s spectra of V-LDPE before and after treatment with the catalyst and NHPI are shown in Figure 27 (a) and 27 (b). The V-LDPE surface was dominated by a C–C/ C–H component at 284.8 eV corresponding to the C-C bond of the polymer backbone. A minor oxidised shoulder peak is seen in C 1s and no discernible O 1s peak, correlating well with the survey spectrum. After 3 h acetolysis, the fraction of C–C/ C–H decreased to ~81 % (from ~99.9 % based on integrated peak area in XPS, in the control), and well-defined oxygenated components emerged in C 1s at ~285.8 eV (C–O), ~287.1 eV (C=O), and ~288.6 eV (O–C=O/ COOR). Correspondingly, O 1s exhibited features at ~532.0 eV (C=O) and ~533.4 eV (O–C=O/COOR), confirming.

clear oxidation of the polymer surface[70]. The assignments are consistent with the FTIR analysis for the sample seen in Figure 27 (c).

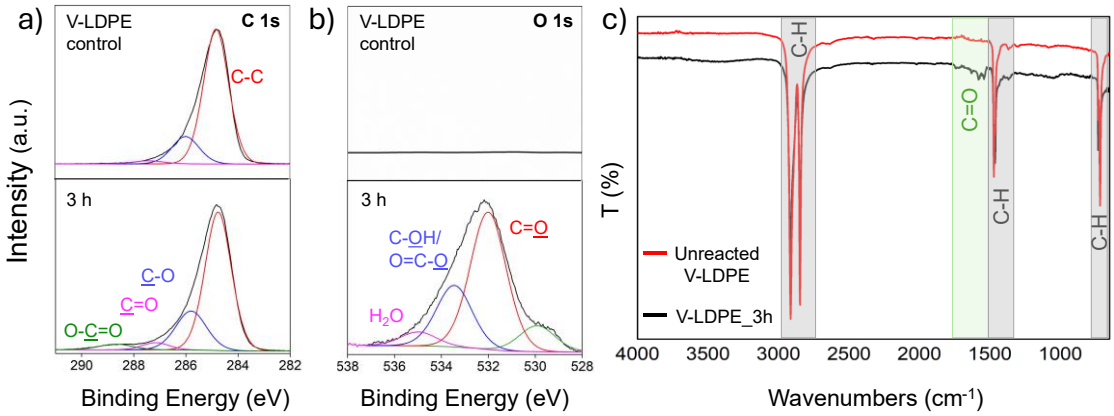


Figure 27. (a) C 1s XPS, **(b)** O 1s XPS and **(c)** FTIR analysis for virgin LDPE before and after a 3 h reaction. All samples have been washed with DI H_2O prior to XPS analysis.

PC-LDPE: chemically diverse surfaces and rapid modification

PC-LDPE exhibited greater surface complexity than V-LPDE (Figure 28). In the PC-LDPE before any reaction, the C 1s and O 1s spectra show components corresponding to aliphatic C-C (284.7 eV) and smaller peaks assigned to oxidised carbon environments: C-O (285.8 eV), C=O (287.0 eV), and O-C=O (288.7 eV) consistent with the nature of the polymer and its additive content. The O 1s region exhibited peaks attributed to carbonyl oxygen: C=O (531.8 eV) and hydroxyl or carboxyl oxygen (533.5 eV)[71]. Following a 15 min acetolysis reaction with both the catalyst and NHPI, the C 1s and O 1s spectrum showed similar peaks while the N 1s peak appeared. The N 1s peaks are assigned to the secondary amine (399.6 eV) and protonated primary amine (401.2 eV) functional groups[72], suggesting the incorporation of NHPI-derived functionalities or the adsorption of NHPI on the surface of the sample. It is unlikely that the nitrogen peaks are attributed to nitrogenous additives as the N 1s spectra

for the PC-LDPE control show signs of nitrogen moieties. Extending the reaction to 3 h produced spectra essentially unchanged from the 15 min sample, indicating that major surface modifications occur rapidly (15 min) and then plateau, which also correlates with the observed mass-loss profiles and FTIR analysis (Figure 28 (d) and (e)). FTIR data exhibits more intense functionalisation at 15 min than at 3 h, exhibiting bands corresponding to N-H and carboxylic acid functionalities.

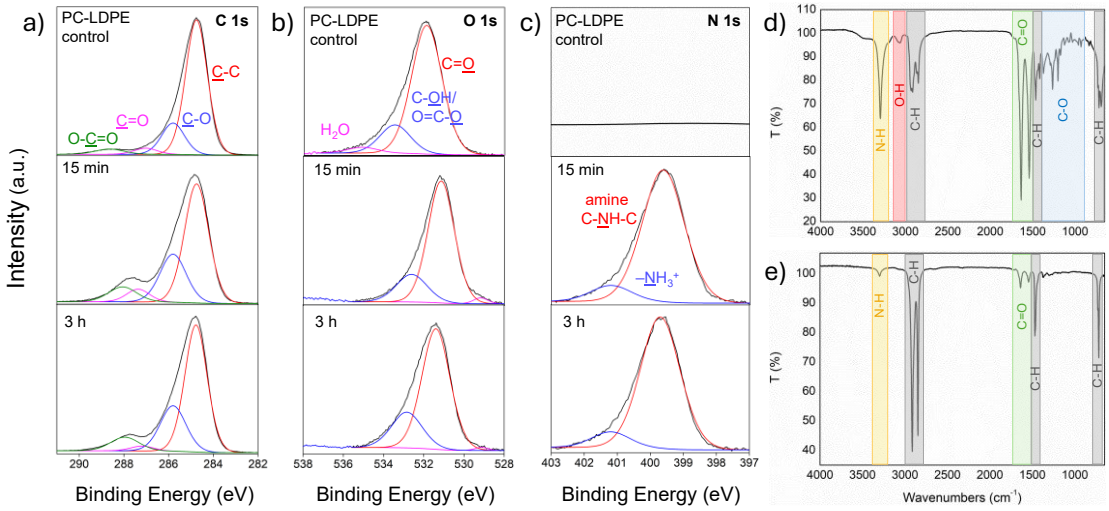


Figure 28. (a) C 1s XPS, **(b)** O 1s XPS and **(c)** N 1s XPS for post-consumer LDPE before reaction and after a 15 min and 3 h reaction. FTIR analysis of PC-LDPE samples after **(d)** 15 min and **(e)** 3 h.

In this work, XPS analysis has provided a detailed understanding of surface chemistry changes during thermo-oxidative degradation on virgin and post-consumer LDPE, particularly in terms of surface functionalisation. The PC-LDPE was markedly more susceptible to the incorporation of surface oxygen and nitrogen-containing groups than V-LDPE, likely due to its processing history, service life and the presence of additives within the PC-LDPE matrix. The pre-existing surface oxidation observed on PC-LDPE seems to facilitate efficiently further chemical degradation rendering the

polymer more reactive towards the acetolysis, with mass loss up to 30 % within 15 min reaction. These results underscore the importance of plastic feedstock history, the importance of interfacial chemistry and additives in plastic packaging that can facilitate polymer degradation pathways.

Conclusions & Outlook

Chapter 4:

4.1 Conclusions

This study demonstrates that the catalyst type, presence of a radical initiator, reagent loadings and the heterogeneity of real-world plastic feedstock strongly influences the course of LDPE acetolysis at 120 °C. From the initial catalyst screening, a heterogeneous Mn-Fe mixed metal catalyst was selected due to its potential bimetallic synergistic effects, materials sustainability and ethical considerations, showing good mass loss performance (30 %), under relatively mild depolymerisation conditions. Time dependent studies revealed differing behaviours for virgin LDPE and post-consumer LDPE with the virgin resin exhibiting resistance to both mass loss and surface functionalisation, whereas the post-consumer LDPE exhibited higher mass loss and pronounced functionalisation, likely influenced by the presence of additives on the surface as well as within the matrix of the polymer.

Systematic variation of catalyst and NHPI loadings demonstrated that these parameters govern both surface oxidation and the diversity of soluble oxidation products. Increasing Mn–Fe loading broadened the HPLC product profile, with formic acid (RT ≈ 17.2 min) consistently dominant. FTIR analysis of the recovered solids showed a general decrease in oxidation intensity at higher catalyst/NHPI loadings, consistent with accelerated oxidative cleavage and desorption of oxygenated fragments rather than their accumulation on the surface.

Finally, re-subjecting previously reacted polymer to a second thermal treatment produced no additional mass loss. Collectively, these observations indicate that under the present solvent temperature, acetic acid and heat alone are sufficient for

partial thermo-oxidative degradation of PC-LDPE, and that catalysis modulates product speciation more than overall conversion. Complementary XPS analysis further supported these findings, showing incorporation of oxygen and nitrogen functionalities on the surface of PC-LDPE within the first 15 min of reaction, whereas the virgin resin remains largely chemically inert with significantly less oxygen incorporation. These surface level insights corroborate the bulk mass loss data and highlight how prior oxidation and additives in post-consumer plastics enhance their susceptibility to thermo-oxidative degradation.

Importantly, the work reported here demonstrates the potential of using acetic acid, a relatively green reagent, for the oxidative degradation of post-consumer LDPE and may be useful in developing a protocol using a mild chemical pretreatment that introduces oxygenated surface functionalities increasing the polymer hydrophilicity, which could be followed by harsher downstream steps e.g. high-pressure oxidation, stronger oxidants, or microwave-assisted redox degradation. Promising results from the surface oxidation of PC-LDPE makes the polymer more susceptible to further degradation through biological or photochemical pathways[73,74]. This study also underscores the necessity of investigating real-world post-consumer plastics whose additives, existing oxidation and processing histories affect kinetics, product distributions and catalyst performance, since conclusions drawn from pristine resins alone may not translate to practical real-world waste streams. The greater extent of oxidation and degradation observed for PC-LDPE is likely attributed to the presence of additives within the polymer matrix and further research is needed to elucidate the precise role of these impurities in driving depolymerisation processes.

4.2 Future Work

Future work should focus on the acetolysis process from two perspectives: (1) optimisation of key reaction parameters (temperature, reaction time, catalyst/NHPI loading) and product analysis and (2) mechanistic understanding of the underlying pathways.

- **Reaction conditions:** An expanded and detailed optimisation on reaction conditions such as temperature, reaction time, and catalyst/NHPI loading. In addition to this, future studies on the role of reaction pressure as well as its influence on mass loss and product distribution could be investigated. While the post-consumer plastic shows good loss, the virgin plastic did not show mass loss, and results from Sullivan *et al.*[22] could not be reproduced. Experiments conducted in an autoclave may shed light on whether elevated pressures increase the rate of depolymerisation or alter product selectivity towards different carboxylic acids.
- **Product analysis:** A particular challenge encountered throughout this work was the quantification of degradation products due to the reaction solvent being acetic acid, which dominated the chromatographic profile. More advanced analytical methods will therefore be necessary to mitigate this complication. Given the low molecular weight, high water solubility, polarity and amphoteric nature of the carboxylic acids, HPLC alone is insufficient. Complementary approaches such as gas chromatography coupled with mass spectrometry (GC-MS) following chemical derivatisation to detect volatile compounds, solid phase extraction (SPE) or dilution to improve peak resolution and the use of a different ion-exclusion phase to improve

resolution of closely eluting acids should be explored to build a more comprehensive picture of the degradation product distribution.

- **Additive-polymer interactions:** Probing how additive chemistry governs initiation and propagation to better understand the mechanistic pathway would be hugely beneficial in designing more efficient depolymerisation protocols. However, this remains challenging as the chemical composition and concentration of the additives are unknown and have considerable variation across different type of plastics (film, packaging, layers plastics, bottles). This presents a key knowledge gap in current research.
- **Process integration:** Explore how the mild acetolysis process developed in this work could be implemented as a pretreatment step preceding more aggressive chemical or thermal treatment to enable higher conversion and improved circularity of post-consumer plastic.

In conclusion, while polyolefins are incredibly versatile polymers with a vast range of applications, a proper understanding of polymer additive chemistry, contamination and degradation mechanisms is needed to pave the way for effective plastics waste upcycling and therefore a sustainable economy. Future research in this field should have broader environmental consideration and prioritise sustainable and green chemistry approaches, including mechanistic studies of polymer-additive interactions, life-cycle assessments of additive-containing products and the development of materials that are degradable by design. Overall, the findings promote circular thinking and reflect an uncompromised commitment to developing sustainable strategies for plastic waste management. By promoting recycling,

optimising resource efficiency by minimising energy consumption and emissions, and valorising plastic waste to decrease landfill accumulation and environmental litter, it is possible to achieve closed production loops and contribute to a circular plastics economy. Innovations in sustainable materials research will catalyse the circular economy, achieving environmental and economic prosperity, laying the foundation for a sustainable future.

Bibliography

(1) Neves, A. Ivory Emulation: The Naturalness of Early Bioinspired Plastics. *Ambix* **2025**, *72* (1), 20–33. https://doi.org/10.1080/00026980.2025.2457914.

(2) Department of Painting, Faculty of Fine Arts, University of the Basque Country (UPV/EHU), Spain; Porcel Ziarsolo, A. Plastics in Fashion: A Review of Plastic Materials in Modern and Contemporary Costume Collections and Their Conservation. *Cons. Património* **2023**. https://doi.org/10.14568/cp27897.

(3) Hahladakis, J. N.; Velis, C. A.; Weber, R.; Iacovidou, E.; Purnell, P. An Overview of Chemical Additives Present in Plastics: Migration, Release, Fate and Environmental Impact during Their Use, Disposal and Recycling. *Journal of Hazardous Materials* **2018**, *344*, 179–199. https://doi.org/10.1016/j.jhazmat.2017.10.014.

(4) PlasticsEurope. *Plastics - the Fast Facts 2024*. https://plasticseurope.org/knowledge-hub/plastics-the-fast-facts-2024/ (accessed 2025-06-26).

(5) Royer, S.-J.; Ferrón, S.; Wilson, S. T.; Karl, D. M. Production of Methane and Ethylene from Plastic in the Environment. *PLoS ONE* **2018**, *13* (8), e0200574. https://doi.org/10.1371/journal.pone.0200574.

(6) MacLeod, M.; Arp, H. P. H.; Tekman, M. B.; Jahnke, A. The Global Threat from Plastic Pollution. *Science* **2021**, *373* (6550), 61–65. https://doi.org/10.1126/science.abg5433.

(7) Rochman, C. M.; Browne, M. A.; Halpern, B. S.; Hentschel, B. T.; Hoh, E.; Karapanagioti, H. K.; Rios-Mendoza, L. M.; Takada, H.; Teh, S.; Thompson, R. C. Classify Plastic Waste as Hazardous. *Nature* **2013**, *494* (7436), 169–171. https://doi.org/10.1038/494169a.

(8) Worm, B.; Lotze, H. K.; Jubinville, I.; Wilcox, C.; Jambeck, J. Plastic as a Persistent Marine Pollutant. *Annu. Rev. Environ. Resour.* **2017**, *42* (1), 1–26. https://doi.org/10.1146/annurev-environ-102016-060700.

(9) Shen, M.; Huang, W.; Chen, M.; Song, B.; Zeng, G.; Zhang, Y. (Micro)Plastic Crisis: Un-Ignorable Contribution to Global Greenhouse Gas Emissions and Climate Change. *Journal of Cleaner Production* **2020**, *254*, 120138. https://doi.org/10.1016/j.jclepro.2020.120138.

(10) Nicholson, S. R.; Rorrer, N. A.; Carpenter, A. C.; Beckham, G. T. Manufacturing Energy and Greenhouse Gas Emissions Associated with Plastics Consumption. *Joule* **2021**, *5* (3), 673–686. https://doi.org/10.1016/j.joule.2020.12.027.

(11) PlasticsEurope. *Plastics - the Facts 2022*; 2022. https://plasticseurope.org/wp-content/uploads/2022/10/PE-PLASTICS-THE-FACTS_V7-Tue_19-10-1.pdf.

(12) Eurostat. Packaging Waste by Waste Management Operations. https://doi.org/10.2908/ENV_WASPAC.

(13) IEA. Statista. *Production Forecast of Thermoplastics Worldwide from 2025 to 2050 (in Million Metric Tons)*; 2020. https://www.statista.com/statistics/664906/plastics-production-volume-forecast-worldwide/ (accessed 2025-03-27).

(14) Schyns, Z. O. G.; Shaver, M. P. Mechanical Recycling of Packaging Plastics: A Review. *Macromol. Rapid Commun.* **2021**, *42* (3). https://doi.org/10.1002/marc.202000415.

(15) Vollmer, I.; Jenks, M. J. F.; Roelands, M. C. P.; White, R. J.; Van Harmelen, T.; De Wild, P.; Van Der Laan, G. P.; Meirer, F.; Keurentjes, J. T. F.; Weckhuysen, B. M. Beyond Mechanical Recycling: Giving New Life to Plastic Waste. *Angew Chem Int Ed* **2020**, *59* (36), 15402–15423. https://doi.org/10.1002/anie.201915651.

(16) Hopewell, J.; Dvorak, R.; Kosior, E. Plastics Recycling: Challenges and Opportunities. *Phil. Trans. R. Soc. B* **2009**, *364* (1526), 2115–2126. https://doi.org/10.1098/rstb.2008.0311.

(17) Liu, Y.; Shi, J.; Jin, H.; Guo, L. Current Research Progress of Physical and Biological Methods for Disposing Waste Plastics. *Journal of Cleaner Production* **2023**, *408*, 137199. https://doi.org/10.1016/j.jclepro.2023.137199.

(18) Jeswani, H.; Krüger, C.; Russ, M.; Horlacher, M.; Antony, F.; Hann, S.; Azapagic, A. Life Cycle Environmental Impacts of Chemical Recycling via Pyrolysis of Mixed Plastic Waste in Comparison with Mechanical Recycling and Energy Recovery. *Science of The Total Environment* **2021**, *769*, 144483. https://doi.org/10.1016/j.scitotenv.2020.144483.

(19) Uekert, T.; Singh, A.; DesVeaux, J. S.; Ghosh, T.; Bhatt, A.; Yadav, G.; Afzal, S.; Walzberg, J.; Knauer, K. M.; Nicholson, S. R.; Beckham, G. T.; Carpenter, A. C. Technical, Economic, and Environmental Comparison of Closed-Loop Recycling Technologies for Common Plastics. *ACS Sustainable Chem. Eng.* **2023**, *11* (3), 965–978. https://doi.org/10.1021/acssuschemeng.2c05497.

(20) Gazzotti, S.; De Felice, B.; Ortenzi, M. A.; Parolini, M. Approaches for Management and Valorization of Non-Homogeneous, Non-Recyclable Plastic Waste. *IJERPH* **2022**, *19* (16), 10088. https://doi.org/10.3390/ijerph191610088.

(21) Vermeulen, I.; Van Caneghem, J.; Block, C.; Baeyens, J.; Vandecasteele, C. Automotive Shredder Residue (ASR): Reviewing Its Production from End-of-Life Vehicles (ELVs) and Its Recycling, Energy or Chemicals' Valorisation. *Journal of Hazardous Materials* **2011**, *190* (1–3), 8–27. https://doi.org/10.1016/j.jhazmat.2011.02.088.

(22) P. Sullivan, K.; Z. Werner, A. Mixed Plastics Waste Valorization through Tandem Chemical Oxidation and Biological Funneling. *Science* **2022**, *378* (6616), 207–211.

(23) Lange, J.-P. Managing Plastic Waste–Sorting, Recycling, Disposal, and Product Redesign. *ACS Sustainable Chem. Eng.* **2021**, *9* (47), 15722–15738. https://doi.org/10.1021/acssuschemeng.1c05013.

(24) Schade, A.; Melzer, M.; Zimmermann, S.; Schwarz, T.; Stoewe, K.; Kuhn, H. Plastic Waste Recycling–A Chemical Recycling Perspective. *ACS Sustainable Chem. Eng.* **2024**, *12* (33), 12270–12288. https://doi.org/10.1021/acssuschemeng.4c02551.

(25) Solis, M.; Silveira, S. Technologies for Chemical Recycling of Household Plastics – A Technical Review and TRL Assessment. *Waste Management* **2020**, *105*, 128–138. https://doi.org/10.1016/j.wasman.2020.01.038.

(26) Ragaert, K.; Delva, L.; Van Geem, K. Mechanical and Chemical Recycling of Solid Plastic Waste. *Waste Management* **2017**, *69*, 24–58. https://doi.org/10.1016/j.wasman.2017.07.044.

(27) Dogu, O.; Pelucchi, M.; Van De Vijver, R.; Van Steenberge, P. H. M.; D'hooge, D. R.; Cuoci, A.; Mehl, M.; Frassoldati, A.; Faravelli, T.; Van Geem, K. M. The Chemistry of Chemical Recycling of Solid Plastic Waste via Pyrolysis and Gasification: State-of-the-Art, Challenges, and Future Directions. *Progress in Energy and Combustion Science* **2021**, *84*, 100901. https://doi.org/10.1016/j.pecs.2020.100901.

(28) Saebea, D.; Ruengrit, P.; Arpornwichanop, A.; Patcharavorachot, Y. Gasification of Plastic Waste for Synthesis Gas Production. *Energy Reports* **2020**, *6*, 202–207. https://doi.org/10.1016/j.egyr.2019.08.043.

(29) Coates, G. W.; Getzler, Y. D. Y. L. Chemical Recycling to Monomer for an Ideal, Circular Polymer Economy. *Nat Rev Mater* **2020**, *5* (7), 501–516. https://doi.org/10.1038/s41578-020-0190-4.

(30) Miao, Y.; Von Jouanne, A.; Yokochi, A. Current Technologies in Depolymerization Process and the Road Ahead. *Polymers* **2021**, *13* (3), 449. https://doi.org/10.3390/polym13030449.

(31) Sambyal, P.; Najmi, P.; Sharma, D.; Khoshbakhti, E.; Hosseini, H.; Milani, A. S.; Arjmand, M. Plastic Recycling: Challenges and Opportunities. *Can J Chem Eng* **2025**, *103* (6), 2462–2498. https://doi.org/10.1002/cjce.25531.

(32) Hyatt JW.; Hyatt IS., . Improvement in Factitious Ivory. 156,354.

(33) Al-Malaika, S.; Axtell, F.; Rothon, R.; Gilbert, M. Additives for Plastics. In *Brydson's Plastics Materials*; Elsevier, 2017; pp 127–168. https://doi.org/10.1016/B978-0-323-35824-8.00007-4.

(34) Andrady, A. L.; Rajapakse, N. Additives and Chemicals in Plastics. In *Hazardous Chemicals Associated with Plastics in the Marine Environment*; Takada, H., Karapanagioti, H. K., Eds.; The Handbook of Environmental Chemistry; Springer International Publishing: Cham, 2016; Vol. 78, pp 1–17. https://doi.org/10.1007/698_2016_124.

(35) Almeida, S.; Ozkan, S.; Gonçalves, D.; Paulo, I.; Queirós, C. S. G. P.; Ferreira, O.; Bordado, J.; Galhano Dos Santos, R. A Brief Evaluation of Antioxidants, Antistatics, and Plasticizers Additives from Natural Sources for Polymers Formulation. *Polymers* **2022**, *15* (1), 6. https://doi.org/10.3390/polym15010006.

(36) Knoben, N.; Vanhouttem, M.; Wypkema, A.; Subramanian, N. Monitoring Antioxidant Consumption and Build-Up in Polypropylene During Open-Loop and Closed-Loop Mechanical Recycling. *Materials* **2025**, *18* (7), 1640. https://doi.org/10.3390/ma18071640.

(37) Pfaendner, R. Polymer Additives. In *Handbook of Polymer Synthesis, Characterization, and Processing*; Saldívar-Guerra, E., Vivaldo-Lima, E., Eds.; Wiley, 2013; pp 225–247. https://doi.org/10.1002/9781118480793.ch11.

(38) Ambrogi, V.; Carfagna, C.; Cerruti, P.; Marturano, V. Additives in Polymers. In *Modification of Polymer Properties*; Elsevier, 2017; pp 87–108. https://doi.org/10.1016/B978-0-323-44353-1.00004-X.

(39) Ajji, A.; Utracki, L. A. Interphase and Compatibilization of Polymer Blends. *Polymer Engineering & Sci* **1996**, *36* (12), 1574–1585. https://doi.org/10.1002/pen.10554.

(40) Maddela, N. R.; Kakarla, D.; Venkateswarlu, K.; Megharaj, M. Additives of Plastics: Entry into the Environment and Potential Risks to Human and Ecological Health. *Journal of Environmental Management* **2023**, *348*, 119364. https://doi.org/10.1016/j.jenvman.2023.119364.

(41) Wiesinger, H.; Wang, Z.; Hellweg, S. Deep Dive into Plastic Monomers, Additives, and Processing Aids. *Environ. Sci. Technol.* **2021**, *55* (13), 9339–9351. https://doi.org/10.1021/acs.est.1c00976.

(42) Deanin R. D. Additives in Plastics. In *Environmental Health Perspectives*; Vol. 11, pp 35–39.

(43) Li, H.; Aguirre-Villegas, H. A.; Allen, R. D.; Bai, X.; Benson, C. H.; Beckham, G. T.; Bradshaw, S. L.; Brown, J. L.; Brown, R. C.; Cecon, V. S.; Curley, J. B.; Curtzwiler, G. W.; Dong, S.; Gaddameedi, S.; García, J. E.; Hermans, I.; Kim, M. S.; Ma, J.; Mark, L. O.; Mavrikakis, M.; Olafasakin, O. O.; Osswald, T. A.; Papanikolaou, K. G.; Radhakrishnan, H.; Sanchez Castillo, M. A.; Sánchez-Rivera, K. L.; Tumu, K. N.; Van Lehn, R. C.; Vorst, K. L.; Wright, M. M.; Wu, J.; Zavala, V. M.; Zhou, P.; Huber, G. W. Expanding Plastics Recycling Technologies: Chemical Aspects, Technology Status and Challenges. *Green Chem.* **2022**, *24* (23), 8899–9002. https://doi.org/10.1039/D2GC02588D.

(44) Hansen, E.; Nilsson, N. H.; Lithner, D.; Lassen, C. Hazardous Substances in Plastic Materials. *COWI in cooperation with Danish Technological Institute* **2013**, 7–8.

(45) Faryal, S.; Zafar, M.; Nazir, M. S.; Ali, Z.; Hussain, M.; Muhammad Imran, S. The Synergic Effect of Primary and Secondary Flame Retardants on the Improvement in the Flame Retardant and Mechanical Properties of Thermoplastic Polyurethane Nanocomposites. *Applied Sciences* **2022**, *12* (21), 10866. https://doi.org/10.3390/app122110866.

(46) Froelich, D.; Maris, E.; Haoues, N.; Chemineau, L.; Renard, H.; Abraham, F.; Lassartesses, R. State of the Art of Plastic Sorting and Recycling: Feedback to Vehicle Design. *Minerals Engineering* **2007**, *20* (9), 902–912. https://doi.org/10.1016/j.mineng.2007.04.020.

(47) Chea, J. D.; Yenkie, K. M.; Stanzione, J. F.; Ruiz-Mercado, G. J. A Generic Scenario Analysis of End-of-Life Plastic Management: Chemical Additives. *Journal of Hazardous Materials* **2023**, *441*, 129902. https://doi.org/10.1016/j.jhazmat.2022.129902.

(48) Teuten, E. L.; Saquing, J. M.; Knappe, D. R. U.; Barlaz, M. A.; Jonsson, S.; Björn, A.; Rowland, S. J.; Thompson, R. C.; Galloway, T. S.; Yamashita, R.; Ochi, D.; Watanuki, Y.; Moore, C.; Viet, P. H.; Tana, T. S.; Prudente, M.; Boonyatumanond, R.; Zakaria, M. P.; Akkhavong, K.; Ogata, Y.; Hirai, H.; Iwasa, S.; Mizukawa, K.; Hagino, Y.; Imamura, A.; Saha, M.; Takada, H. Transport and Release of Chemicals from Plastics to the Environment and to Wildlife. *Phil. Trans. R. Soc. B* **2009**, *364* (1526), 2027–2045. https://doi.org/10.1098/rstb.2008.0284.

(49) Paluselli, A.; Fauvelle, V.; Galgani, F.; Sempéré, R. Phthalate Release from Plastic Fragments and Degradation in Seawater. *Environ. Sci. Technol.* **2019**, *53* (1), 166–175. https://doi.org/10.1021/acs.est.8b05083.

(50) Singkronart, K.; Virkajärvi, J.; Salminen, K.; Shamsuddin, S. R.; Lee, K.-Y. Immiscible Polymer Blends Made from Industrial Shredder Residue Mixed Plastic *with* and *without* Melt Blending. *ACS Appl. Polym. Mater.* **2024**, *6* (11), 6252–6261. https://doi.org/10.1021/acsapm.4c00360.

(51) Ausili, A.; Sánchez, M.; Gómez-Fernández, J. C. Attenuated Total Reflectance Infrared Spectroscopy: A Powerful Method for the Simultaneous Study of Structure and Spatial Orientation of Lipids and Membrane Proteins. *Biomedical Spectroscopy and Imaging* **2015**, *4* (2), 159–170. https://doi.org/10.3233/bsi-150104.

(52) S. Mitchell. *X-Ray Photoelectron Spectroscopy*; 2025. https://www.eag.com/techniques/spectroscopy/x-ray-photoelectron-spectroscopy-xps-esca/ (accessed 2025-07-24).

(53) Bäckström, E.; Odelius, K.; Hakkarainen, M. Trash to Treasure: Microwave-Assisted Conversion of Polyethylene to Functional Chemicals. *Ind. Eng. Chem. Res.* **2017**, *56* (50), 14814–14821. https://doi.org/10.1021/acs.iecr.7b04091.

(54) Haidar Ahmad, I. Studying Chemical and Sequence Length Heterogeneities in Copolymers, 2011.

(55) Farahmandjou, M.; Soflaee, F. Synthesis and Characterization of α-Fe2O3 Nanoparticles by Simple Co-Precipitation Method. *PCR* **2015**, *3* (3). https://doi.org/10.22036/pcr.2015.9193.

(56) Breen, R.; Holmes, J. D.; Collins, G. Heterogeneous Fenton-Type Oxidative Degradation of Low-Density Polyethylene to Valuable Acid Products Using a Nanostructured Fe–CeO_2 Solid Solution Catalyst. *Catal. Sci. Technol.* **2025**, *15* (3), 920–932. https://doi.org/10.1039/d4cy01384k.

(57) Wu, R.; Qu, J.; He, H.; Yu, Y. Removal of Azo-Dye Acid Red B (ARB) by Adsorption and Catalytic Combustion Using Magnetic CuFe2O4 Powder. *Applied Catalysis B: Environmental* **2004**, *48* (1), 49–56. https://doi.org/10.1016/j.apcatb.2003.09.006.

(58) Tomás, R. A. F.; Bordado, J. C. M.; Gomes, J. F. P. *P*-Xylene Oxidation to Terephthalic Acid: A Literature Review Oriented toward Process Optimization and Development. *Chem. Rev.* **2013**, *113* (10), 7421–7469. https://doi.org/10.1021/cr300298j.

(59) Ishii, Y.; Iwahama, T.; Sakaguchi, S.; Nakayama, K.; Nishiyama, Y. Alkane Oxidation with Molecular Oxygen Using a New Efficient Catalytic System: *N*-Hydroxyphthalimide (NHPI) Combined with $Co(Acac)_n$(*n*= 2 or 3). *J. Org. Chem.* **1996**, *61* (14), 4520–4526. https://doi.org/10.1021/jo951970l.

(60) Plekhov, A. L.; Kushch, O. V.; Opeida, I. O.; Kompanets, M. A. Catalytic Oxidation of P-Xylene with Molecular Oxygen in the Presence of N-Hydroxyphthalimide. *Russ J Appl Chem* **2014**, *87* (7), 982–985. https://doi.org/10.1134/s1070427214070222.

(61) Partenheimer, W. Methodology and Scope of Metal/Bromide Autoxidation of Hydrocarbons. *Catalysis Today* **1995**, *23* (2), 69–158. https://doi.org/10.1016/0920-5861(94)00138-r.

(62) Opeida, I. A.; Plekhov, A. L.; Kushch, O. V.; Matvienko, A. G. Complexes of N-Hydroxyphthalimide and Cobalt(II) Acetate in Reactions of Alkylarene Oxidation by Molecular Oxygen. *Russ. J. Phys. Chem.* **2011**, *85* (7), 1119–1123. https://doi.org/10.1134/s0036024411070247.

(63) Hara, T.; Iwahama, T.; Sakaguchi, S.; Ishii, Y. Catalytic Oxyalkylation of Alkenes with Alkanes and Molecular Oxygen via a Radical Process Using *N*-Hydroxyphthalimide. *J. Org. Chem.* **2001**, *66* (19), 6425–6431. https://doi.org/10.1021/jo0157977.

(64) Smith, B. C. The Infrared Spectra of Polymers II: Polyethylene. *Spectroscopy* **2021**, 24–29. https://doi.org/10.56530/spectroscopy.xp7081p7.

(65) Almond, J.; Sugumaar, P.; Wenzel, M. N.; Hill, G.; Wallis, C. Determination of the Carbonyl Index of Polyethylene and Polypropylene Using Specified Area under Band Methodology with ATR-FTIR Spectroscopy. *e-Polymers* **2020**, *20* (1), 369–381. https://doi.org/10.1515/epoly-2020-0041.

(66) Bracco, P.; Costa, L.; Luda, M. P.; Billingham, N. A Review of Experimental Studies of the Role of Free-Radicals in Polyethylene Oxidation. *Polymer Degradation and Stability* **2018**, *155*, 67–83. https://doi.org/10.1016/j.polymdegradstab.2018.07.011.

(67) Zeng, S.; Lu, D.; Yang, R. Effects of Crystallinity and Branched Chain on Thermal Degradation of Polyethylene: A SCC-DFTB Molecular Dynamics Study. *Polymers* **2024**, *16* (21), 3038. https://doi.org/10.3390/polym16213038.

(68) Niu, L.; Shen, J.; Li, Y.; Chen, Y.; Zhang, W.; Wang, L. Plastic Additives Alter the Influence of Photodegradation on Biodegradation of Polyethylene/Polypropylene Polymers in Natural Rivers. *Journal of Hazardous Materials* **2025**, *489*, 137542. https://doi.org/10.1016/j.jhazmat.2025.137542.

(69) Sun, J.; Dong, J.; Gao, L.; Zhao, Y.-Q.; Moon, H.; Scott, S. L. Catalytic Upcycling of Polyolefins. *Chem. Rev.* **2024**, *124* (16), 9457–9579. https://doi.org/10.1021/acs.chemrev.3c00943.

(70) Briggs, D.; Brewis, D. M.; Dahm, R. H.; Fletcher, I. W. Analysis of the Surface Chemistry of Oxidized Polyethylene: Comparison of XPS and ToF-SIMS. *Surface & Interface Analysis* **2003**, *35* (2), 156–167. https://doi.org/10.1002/sia.1515.

(71) Bag, D. S.; Ghosh, S. N.; Maiti, S. Surface Modification and Evaluation of Polyethylene Film. *European Polymer Journal* **1998**, *34* (5–6), 855–861. https://doi.org/10.1016/S0014-3057(97)00178-X.

(72) Yu, B.; Wang, X.; Qian, X.; Xing, W.; Yang, H.; Ma, L.; Lin, Y.; Jiang, S.; Song, L.; Hu, Y.; Lo, S. Functionalized Graphene Oxide/Phosphoramide Oligomer Hybrids Flame Retardant Prepared via in Situ Polymerization for Improving the Fire Safety of Polypropylene. *RSC Adv.* **2014**, *4* (60), 31782. https://doi.org/10.1039/C3RA45945D.

(73) Arnaud, R.; Dabin, P.; Lemaire, J.; Al-Malaika, S.; Chohan, S.; Coker, M.; Scott, G.; Fauve, A.; Maaroufi, A. Photooxidation and Biodegradation of Commercial Photodegradable Polyethylenes. *Polymer Degradation and Stability* **1994**, *46* (2), 211–224. https://doi.org/10.1016/0141-3910(94)90053-1.

(74) Zhu, Y.; Wang, H.; Bai, J.; Qi, Y.; Han, D. Biodegradation Potential of Gordonia Spp. on Polypropylene and Polystyrene: Enhanced Degradation through Pretreatment. *Front. Microbiol.* **2025**, *16*, 1621498. https://doi.org/10.3389/fmicb.2025.1621498.